

**DOT/FAA/AR-98/33**

Office of Aviation Research  
Washington, D.C. 20591

# **Uniaxial and Biaxial Tests on Riveted Fuselage Lap Joint Specimens**

October 1998

Final Report

This document is available to the U.S. public  
Through the National Technical Information  
Service (NTIS), Springfield, Virginia 22161.



U.S. Department of Transportation  
**Federal Aviation Administration**

## **NOTICE**

This document is disseminated under the sponsorship of the U.S. Department of Transportation in the interest of information exchange. The United States Government assumes no liability for the contents or use thereof. The United States Government does not endorse products or manufacturers. Trade or manufacturer's names appear herein solely because they are considered essential to the objective of this report.

1. Report No. DOT/FAA/AR-98/33		2. Government Accession No.		3. Recipient's Catalog No.	
4. Title and Subtitle  UNIAXIAL AND BIAXIAL TESTS ON RIVETED FUSELAGE LAP JOINT SPECIMENS				5. Report Date October 1998	
				6. Performing Organization Code	
7. Author(s) H. Vlieger and H.H. Ottens				8. Performing Organization Report No. NLR CR 97319L	
9. Performing Organization Name and Address Nationaal Luch-En Ruimtevaart Laboratorium National Aerospace Laboratory NLR 1059 CM Amsterdam, PO Box 90502 The Netherlands				10. Work Unit No. (TRAIS)	
				11. Contract or Grant No. MoC AIA/CA-52-3-2	
12. Sponsoring Agency Name and Address U.S. Department of Transportation Federal Aviation Administration Office of Aviation Research Washington, DC 20591				13. Type of Report and Period Covered Final Report	
				14. Sponsoring Agency Code AAR-430	
15. Supplementary Notes FAA William J. Hughes Technical Center monitor: Dr. Paul Tan					
16. Abstract  As a part of a collaboration program between the Federal Aviation Administration (FAA, USA) and the Department of Civil Aviation (RLD, the Netherlands), the Dutch National Aerospace Laboratory (NLR) has carried out fatigue tests on riveted lap joint specimens. The specimens are representative of the longitudinal lap joints of a commercial aircraft in which multiple-site damage (MSD) was found in service. Two different rivet configurations, dimpled and countersunk riveted joints, were investigated. The countersunk riveted specimens were bonded as well. Four different bonding qualities ranging from fully bonded to fully unbonded were tested.  The results of the test program showed that the fatigue life until failure of the dimpled lap joint specimens was about one-quarter of that of the unbonded countersunk specimens. The bonding quality is a major parameter for the fatigue life. Fully or partly bonded specimens did not show fatigue cracking within 500 or even 1000 kilocycles. Specimens with a fully degraded bonding layer have slightly better fatigue properties compared to fully unbonded specimens.					
17. Key Words Dimpled rivet joints, Countersunk rivet joints, Lap joint specimens, Bonding quality			18. Distribution Statement This document is available to the public through the National Technical Information Service (NTIS), Springfield, Virginia 22161.		
19. Security Classif. (of this report) Unclassified		20. Security Classif. (of this page) Unclassified		21. No. of Pages 56	22. Price N/A

## TABLE OF CONTENTS

	Page
EXECUTIVE SUMMARY	vii
1. INTRODUCTION	1
2. DESCRIPTION OF THE TEST PROGRAM	1
3. DESCRIPTION OF THE SPECIMENS	11
4. EXECUTION OF THE TESTING	11
4.1 Uniaxial Tests	11
4.2 Biaxial Tests	14
5. SPATE MEASUREMENT PERFORMED	18
6. RESULTS OF TESTS AND MEASUREMENTS	18
7. DISCUSSION	45
7.1 General Remarks	45
7.2 Comparison of Countersunk Riveted and Dimpled Riveted Lap Joints	46
7.3 The Effect of the Bonding Quality	47
7.4 Comparison of Wide- and Narrow-Specimen Results	48
8. CONCLUSIONS	48
9. REFERENCES	49

## LIST OF FIGURES

Figure		Page
1	Structural Details of Longitudinal Skin Splices With Multiple-Site Damage	2
2	Configuration for 120-mm-Wide Lap Joint Specimens	5
3	Configuration for 160-mm-Wide Lap Joint Specimens	6
4	Configuration for 480-mm-Wide Countersunk Lap Joint Speicmens	8
5a	Configuration for 480-mm-Wide Dimpled Lap Joint Speicmens (D4a, D5a)	9
5b	Configuration for 480-mm-Wide Dimpled Lap Joint Speicmens (D3a)	10
6	Exploded View of 160-mm-Wide Biaxial Lap Joint Specimen	12
7	Position of Strain Gauges on 160-mm-Wide Lap Joint Specimens	13
8a	Biaxial Test Setup	14
8b	One of the 480-mm-Wide Biaxial Specimens Mounted in the Test Frame	17
8c	Positions of Strain Guages on Specimen to Realize a Correct Alignment During the Test	18
9	Results for Specimen C1c	21
10	Results for Specimen C2c	21
11	Results for Specimen C3c	22
12	Results for Specimen C4c	22
13	Results for Specimen C5c	23
14	Results for Specimen C2a	23
15	Results for Specimen C4d	24
16	Results for Specimen C5d	24
17	Results for Specimen C1e	25
18	Results for Specimen C2e	26
19	Results for Specimen C3e	27

20	Results for Specimen C4e	28
21	Results for Specimen C5e	29
22	Results for Specimen C1a	30
23	Results for Specimen C3a	31
24	Results for Specimen C4f	32
25	Results for Specimen C5f	33
26	Results for Specimen C4a	34
27	Results for Specimen C5a	36
28	Results for Specimen C6a	38
29	Results for Specimen D3a	40
30	Results for Specimen D4a	42
31	Results for Specimen D5a	43
32	Results of SPATE Measurements	45

#### LIST OF TABLES

Table		Page
1a	Original Test Program on Riveted/Bonded Fuselage Lap Joint Specimens	3
1b	Actual Test Program on Fuselage Lap Joint Specimens	4
2	Summary of Applied Loads	16
3	Summary of the Test Results	19
4	Diameter (mm) of the Rivet Formed Head for the Rivets in the Critical Row	20

## EXECUTIVE SUMMARY

As a part of a collaboration program between the Federal Aviation Administration (FAA, USA) and the Department of Civil Aviation (RLD, the Netherlands), the Dutch National Aerospace Laboratory (NLR) has carried out fatigue tests on riveted lap joint specimens. The specimens are representative of the longitudinal lap joints of a commercial aircraft in which multiple-site damage (MSD) was found in service. Two different rivet configurations, dimpled and countersunk riveted joints, were investigated. The countersunk riveted specimens were bonded as well. Four different bonding qualities ranging from fully bonded to fully unbonded were tested.

The results of the test program showed that the fatigue life until failure of the dimpled lap joint specimens was about one-quarter of that of the unbonded countersunk specimens. The bonding quality is a major parameter for the fatigue life. Fully or partly bonded specimens did not show fatigue cracking within 500 or even 1000 kilocycles. Specimens with a fully degraded bonding layer have slightly better fatigue properties compared to fully unbonded specimens.

## 1. INTRODUCTION.

The Federal Aviation Administration (FAA, USA) and the Department of Civil Aviation (RLD, the Netherlands) have defined a collaborative program on structural integrity of aging aircraft. As part of this program the Dutch National Aerospace Laboratory (NLR) carried out fatigue tests on riveted lap joint specimens.

In the first part of this test program, specimens designed and manufactured in the USA were tested uniaxially and biaxially. The results of these tests have been reported in references 1 and 2.

In the second part, specimens tested were representative of a fuselage longitudinal lap joint of a commercial aircraft with multiple-site damage (MSD) (see figure 1). Two different rivet configurations were used: two rows with dimpled rivets and three rows with countersunk rivets. The countersunk riveted joints were cold bonded as well. The quality of the bonding was evaluated in the test program. Four bonding qualities were investigated: fully bonded, partly bonded (simulating manufacturing defects), degraded bonding (simulating bonding degradation during service), and fully unbonded. Different specimen widths (120, 160, and 480 mm) were used. The specimens were loaded either uniaxially or biaxially. All specimens were manufactured by Fokker Aircraft Corporation in order to guarantee aircraft manufacturer quality.

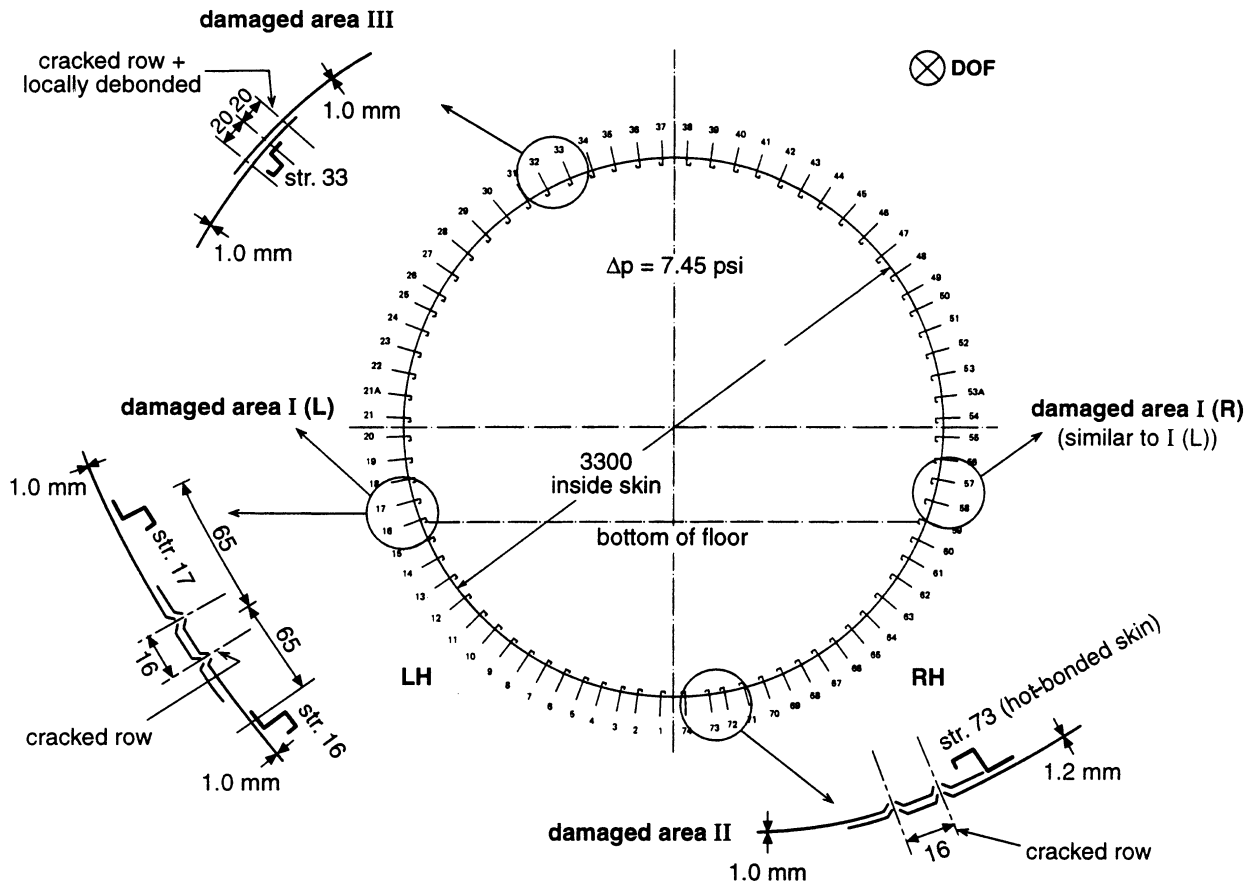
In this report the test program (section 2), the specimens (section 3), the execution of the tests (section 4), the measurement (section 5), and the test results (section 6) are described. The test results are discussed in section 7 and the conclusions are presented in section 8.

## 2. DESCRIPTION OF THE TEST PROGRAM.

The test program, as originally planned, is summarized in table 1a. Two specimen widths were planned. The wide specimens (480 mm) had dimpled (without bonding) or countersunk (fully or partly bonded) rivet connections. All narrow specimens (160 mm) contained a countersunk/bonded rivet connection (with various degrees of debonding of the bonding layer, see below).

The test program performed was slightly different from the test program originally planned (table 1a), as given in table 1b.

**Cross Section of Fuselage (Typical)  
and Stiffener Numbering System**



**Note:** the damaged areas are positioned at different longitudinal fuselage stations

damaged area	rivet connection in damaged lap joints	
	I	dimpled <i>(not bonded and no interfaying sealant)</i>
II	countersunk and cold bonded (EC 2216)	three rows of NAS 1097 AD4 rivets, pitch 20 mm

C428-01N

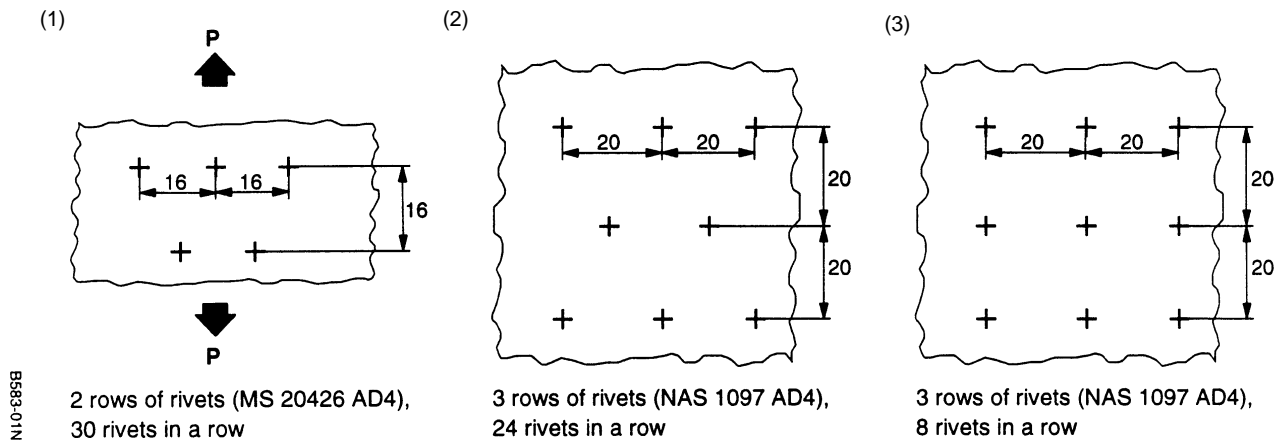
FIGURE 1. STRUCTURAL DETAILS OF LONGITUDINAL SKIN SPLICES WITH MULTIPLE-SITE DAMAGE

TABLE 1a. ORIGINAL TEST PROGRAM ON RIVETED/BONDED FUSELAGE LAP JOINT SPECIMENS (SEE FIGURE 1)

Specimen Configuration		Width (mm)	Number of Specimens	Biaxial/Uniaxial Specimens	Stress Level (C-A)
Dimpled (1)	Not Bonded, No Interfaying Sealant	480	3	Biaxial	$\sigma_{\max} = 94 \text{ MPa}$ $R = 0.10$
Countersunk + Bonded (2)	No Debonding		3		
	Partially Debonded*		3		
Countersunk + Bonded (2)	Fully Bonded	160	3	In Each Group: 2 Uniaxial, 1 Biaxial	
	Partially Debonded		3		
	Bonded, Separated, and Riveted		3		
	Fully Debonded		3		

\*Amount of debonding to be applied in specimens based on test results obtained from 160-mm-wide specimens.

**Rivet pattern:**



**Note: All dimensions are in mm**

One of the purposes of the test program was to investigate the influence of the bonding quality on the fatigue life of the riveted and bonded lap joints. Four bonding quality conditions were tested on the narrow specimens:

- Fully bonded joint.
- Partly bonded to simulate manufacturing errors.
- Fully bonded, then torn apart and riveted again to simulate bonding degradation in service.
- Fully unbonded.

TABLE 1b. ACTUAL TEST PROGRAM ON FUSELAGE LAP JOINT SPECIMENS

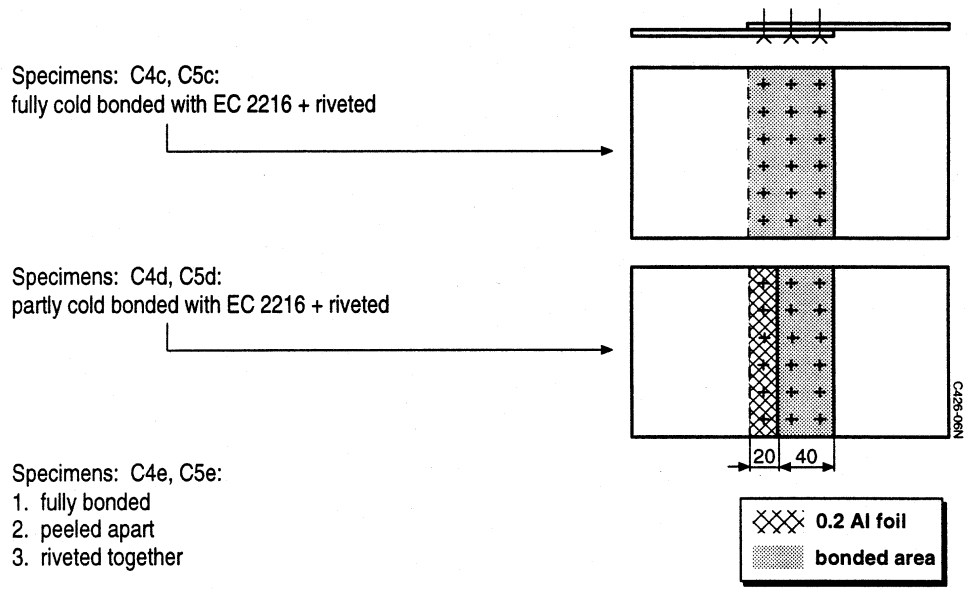
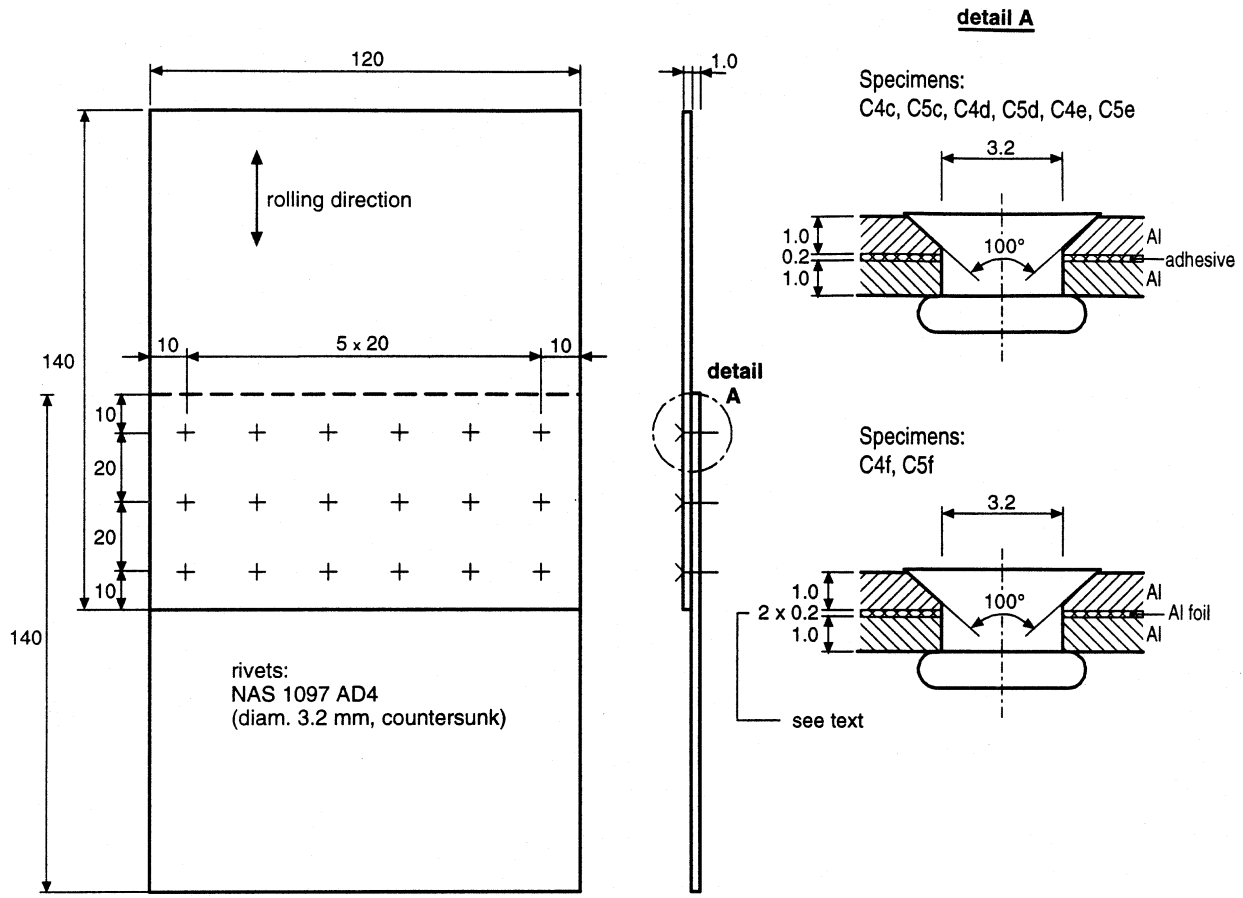
Specimen No.	Specimen Width (mm)	Bonding Quality	Loading Uniaxial/Biaxial	Rivet Type
C1c	160	fully bonded	biaxial	countersunk
C2c	160	fully bonded	uniaxial	countersunk
C3c	160	fully bonded	uniaxial	countersunk
C4c	120	fully bonded	uniaxial	countersunk
C5c	120	fully bonded	biaxial	countersunk
C2a	480	fully bonded	biaxial	countersunk
C4d	120	partly bonded	uniaxial	countersunk
C5d	120	partly bonded	biaxial	countersunk
C1e	160	degradation of bonding <sup>1</sup>	uniaxial	countersunk
C2e	160	degradation of bonding <sup>1</sup>	uniaxial	countersunk
C3e	160	degradation of bonding <sup>1</sup>	biaxial	countersunk
C4e	120	degradation of bonding <sup>1</sup>	uniaxial	countersunk
C5e	120	degradation of bonding <sup>1</sup>	biaxial	countersunk
C1a	480	degradation of bonding <sup>1</sup>	biaxial	countersunk
C3a	480	degradation of bonding <sup>1</sup>	biaxial	countersunk
C4f	120	unbonded <sup>2</sup>	uniaxial	countersunk
C5f	120	unbonded <sup>2</sup>	biaxial	countersunk
C4a	480	unbonded <sup>3</sup>	biaxial	countersunk
C5a	480	unbonded	biaxial	countersunk
C6a	480	unbonded	biaxial	countersunk
D3a	480	unbonded	biaxial	dimpled
D4a	480	unbonded	biaxial	dimpled
D5a	480	unbonded	biaxial	dimpled

<sup>1</sup> Fully bonded, then torn apart and riveted again.

<sup>2</sup> With 2- x 0.2-mm-thick aluminum foil (see figure 2).

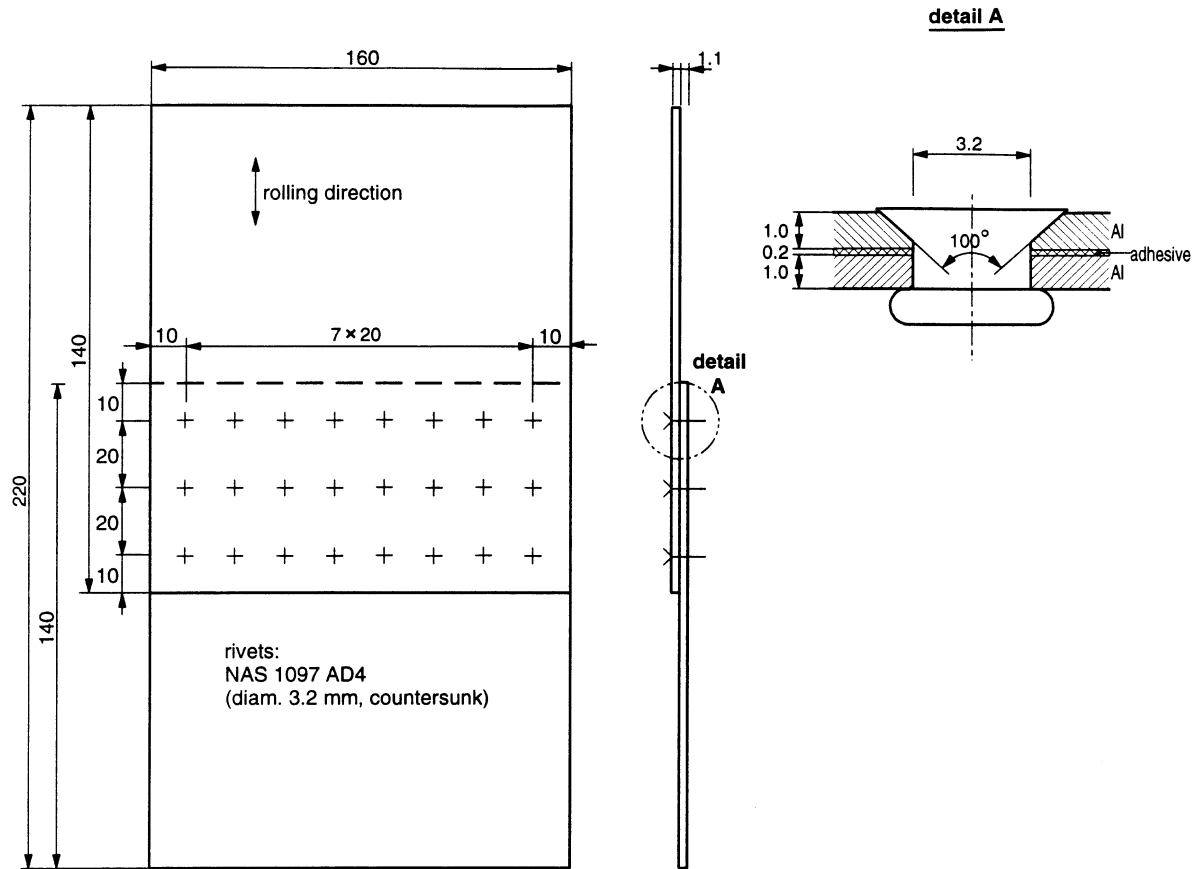
<sup>3</sup> With 0.2-mm-thick aluminum foil (see figure 4).

Three specimens were planned (160 mm in width) for each bonding condition (see table 1a and figure 3).



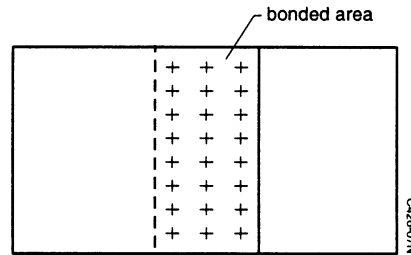
Note: All dimensions are in mm

FIGURE 2. CONFIGURATION FOR 120-mm-WIDE LAP JOINT SPECIMENS



Specimens: C1c, C2c, C3c:  
fully cold bonded with EC 2216 + riveted

Specimens: C1e, C2e, C3e:  
1. fully cold bonded with EC 2216  
2. peeled apart (destroying the bond)  
3. riveted together again



Note: All dimensions are in mm

FIGURE 3. CONFIGURATION FOR 160-mm-WIDE LAP JOINT SPECIMENS

All specimens, however, were delivered fully bonded rather than with the different bonding conditions.

Six of the specimens were used for the following bonding conditions (see table 1b): fully bonded specimens C1c, C2c, and C3c and bonding degradation specimens C1e, C2e, and C3e.

New specimens were manufactured, two specimens for each bonding quality condition. These specimens, however, were made 120 mm wide instead of the 160 mm, but all bonding conditions were applied correctly (see table 1b and figure 2):

- a. Fully bonded specimens C4c and C5c.
- b. Partly bonded specimens C4d and C5d.
- c. Bonding degradation specimens C4e and C5e.
- d. Unbonded specimens C4f and C5f.

The unbonded specimens were designed so that a thin aluminium sheet (0.2 mm thick) was placed between the riveted sheets so that the specimens would have the same joint thickness as the bonded configurations. This was thought to be important in order to have the same secondary bending in the specimens for the different bonding conditions. However, in specimens C4f and C5f, two foils of 0.2 mm thickness were used instead of one (see figure 2). In the partly bonded specimens C4d and C5d, a 0.2-mm-thick aluminium foil (see figure 2) was used in the unbonded part.

Some of the narrow specimens (120 and 160 mm wide) were tested uniaxially, the rest were tested biaxially. All wide specimens (480 mm) were tested biaxially (see table 1b).

On the basis of the test results obtained from the narrow specimens, it was decided to use the six 480-mm-wide specimens with countersunk rivets to test the following bonding conditions (see table 1b and figure 4):

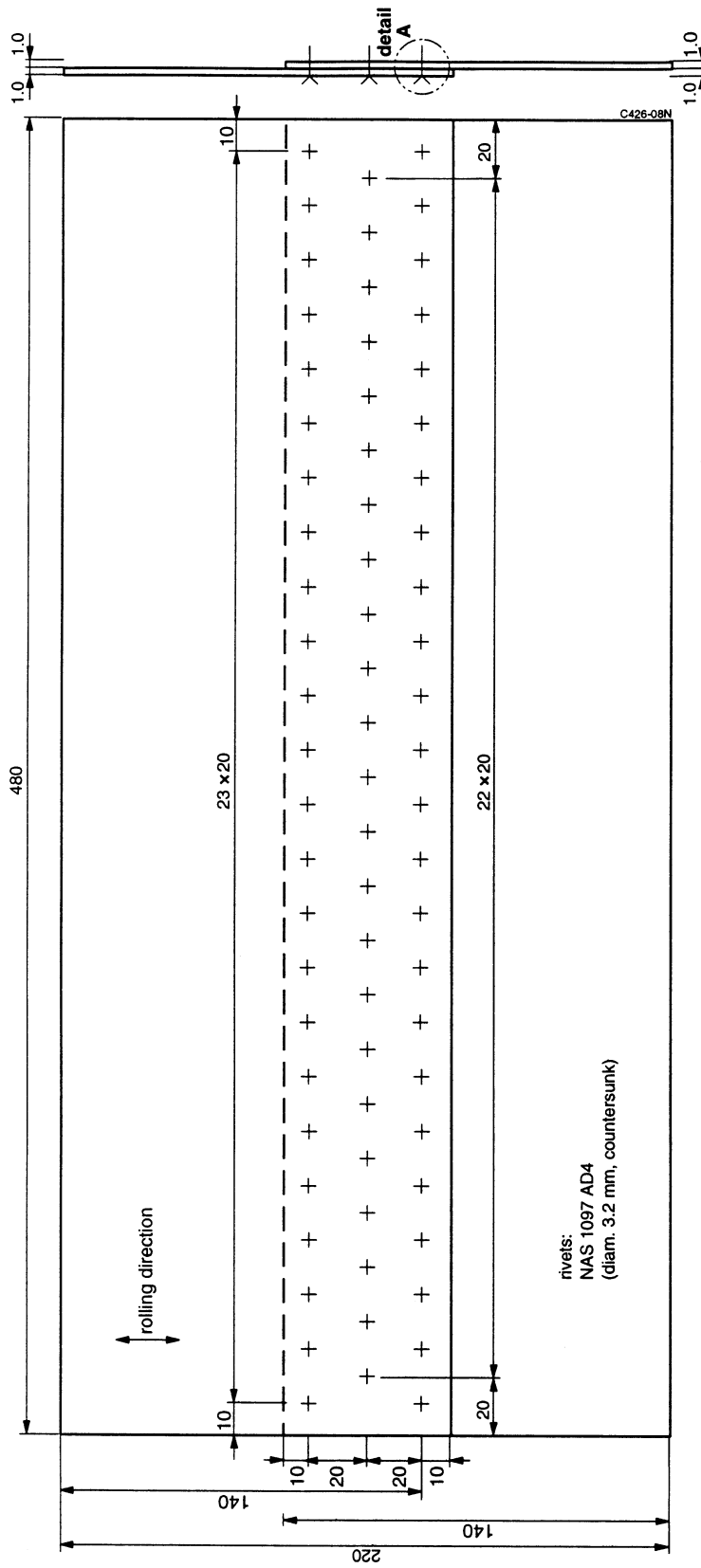
- a. Fully bonded, only one specimen, C2a, for reference purposes.
- b. Bonding degradation specimens C1a, C3a.
- c. Unbonded specimens C4a, C5a, and C6a.

In specimen C4a, a thin aluminium sheet (0.2 mm thick) was inserted between the specimen halves for reasons discussed previously. In specimens C5a and C6a this sheet was omitted.

The 480-mm-wide specimens with dimpled riveted joints were numbered D3a, D4a, and D5a (see table 1b and figures 5a and 5b).

All wide specimens (countersunk riveted and dimpled riveted) were tested biaxially only.

In addition to the specimens used in the testing program, 480-mm-wide dimpled and countersunk lap joint specimens were manufactured to serve as calibration specimens for the eddy-current inspections to be carried out during the tests. For that purpose these specimens were provided with artificial defects (EDM-electrical discharge machined notches) representing fatigue cracks initiated in or near the lap joint rivet holes. For more details about these specimens see reference 3.



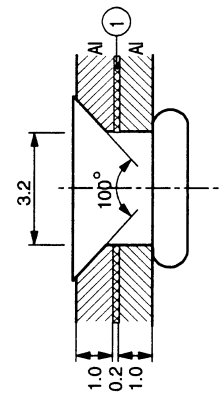
rivets:  
NAS 1097 AD4  
(diam. 3.2 mm, countersunk)

Specimens: C2a : fully bonded with EC 2216 + riveted

Specimens: C1a, C3a : fully bonded, peeled apart riveted again

Specimens: C4a, C5a, C6a : fully unbonded riveted only

Note: All dimensions are in mm

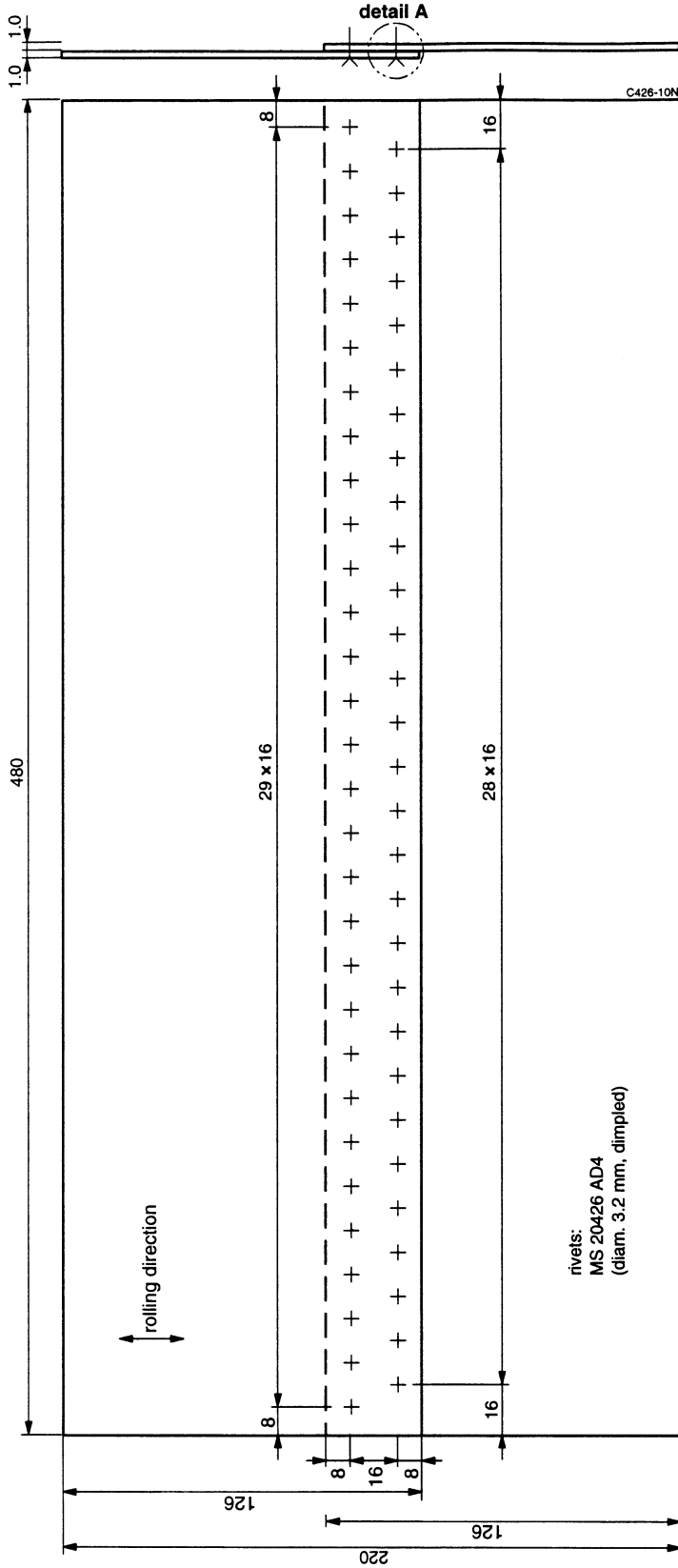


① Specimens : C1a, C2a, C3a : 0.2 mm adhesive  
Specimen : C4a : 0.2 mm Al foil  
Specimens : C5a, C6a : nothing

detail A

FIGURE 4. CONFIGURATION FOR 480-mm-WIDE COUNTERSUNK LAP JOINT SPECIMENS





Specimen: D3a

Note: All dimensions are in mm

FIGURE 5b. CONFIGURATION FOR 480-mm-WIDE DIMPLED LAP JOINT SPECIMENS (D3a)

### 3. DESCRIPTION OF THE SPECIMENS.

As discussed in the previous section, several specimen widths were used: 120, 160, and 480 mm. Specimen dimensions and details are given in figures 2 to 6.

All specimens were made of 1-mm-thick aluminium alloy 2024-T3 alclad material. Prior to assembling the two parts of the specimens, the specimen parts were pretreated, anodized, and primed according to industrial specifications. The (cold) adhesive used was EC2216. The rivets used were NAS 1097 AD4 for the countersunk specimens and MS 20426 AD4 for the dimpled specimens, both with a 3.2 mm diameter.

The dimpled specimens had two rivet rows in a staggered configuration. One row has 30 rivets, the other 29 rivets. The 29-rivet row for specimens D4a and D5a and the 30-rivet row for specimen D3a is at the highly loaded countersunk side as is shown in figures 5a and 5b.

After delivery to NLR, the specimens for uniaxial testing were placed in the clamping area with 1-mm-thick aluminium tabs (at either side) to prevent clamping failure.

The specimens for biaxial testing required special treatment. To be able to run biaxial fatigue tests on specimens in which the lap joint is the fatigue critical area, special attention must be paid to the load introduction into the lap joint area. Figure 6 shows how the biaxial loads were introduced into the test section by means of clamping arms consisting of either unidirectional aramid fibers embedded in epoxy resin (with the narrow specimens for both loading directions and with the wide specimens for the loading direction parallel to the lap joint) or unidirectional glass fibers only (with the wide specimens for the loading direction normal to the lap joint). These arms were cold bonded to the four specimen edges.

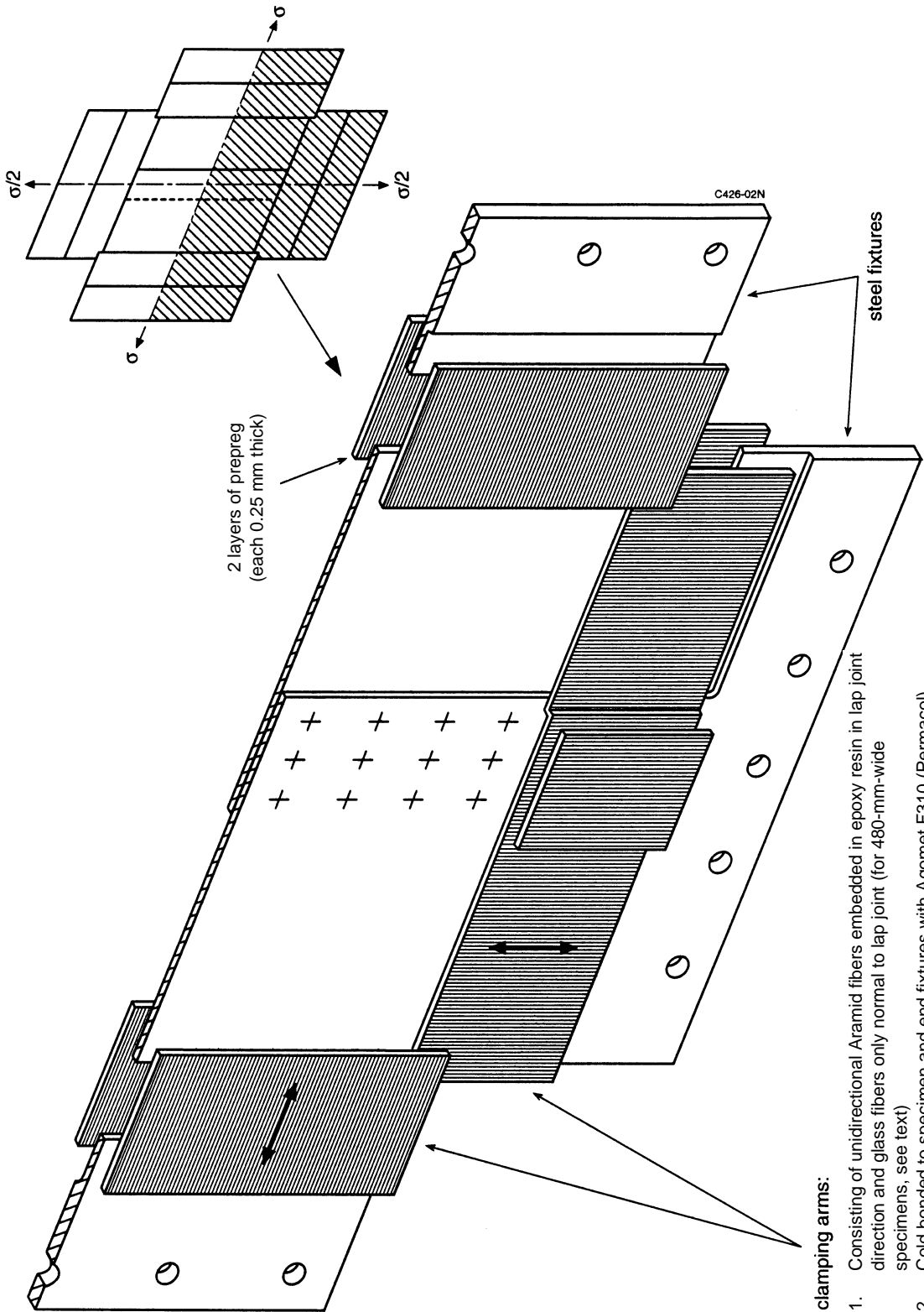
### 4. EXECUTION OF THE TESTING.

#### 4.1 UNIAXIAL TESTS.

The uniaxial constant amplitude fatigue tests were carried out in a 350 kN MTS servo-hydraulic testing machine. The maximum stress levels were nominally 94 MPa. An R-ratio (ratio of minimum-to-maximum stress in a cycle) of 0.1 was used. In this way the stress range ( $\Delta\sigma$ ) in the tests corresponded to a  $\sigma_{\text{hoop}}$  of 85 MPa, a stress value typical for the cabin differential pressure of a midsize commercial aircraft. The actual applied stress levels and the resulting specimen end loads are given in table 2. A chord range of 50 kN of the testing machine was used for these tests.

All tests were carried out under load control at a frequency of 10 Hz. At that frequency no dynamic effects were experienced so that no special fixturing was required.

The specimen ends were clamped in standard clamping devices of the testing machine.

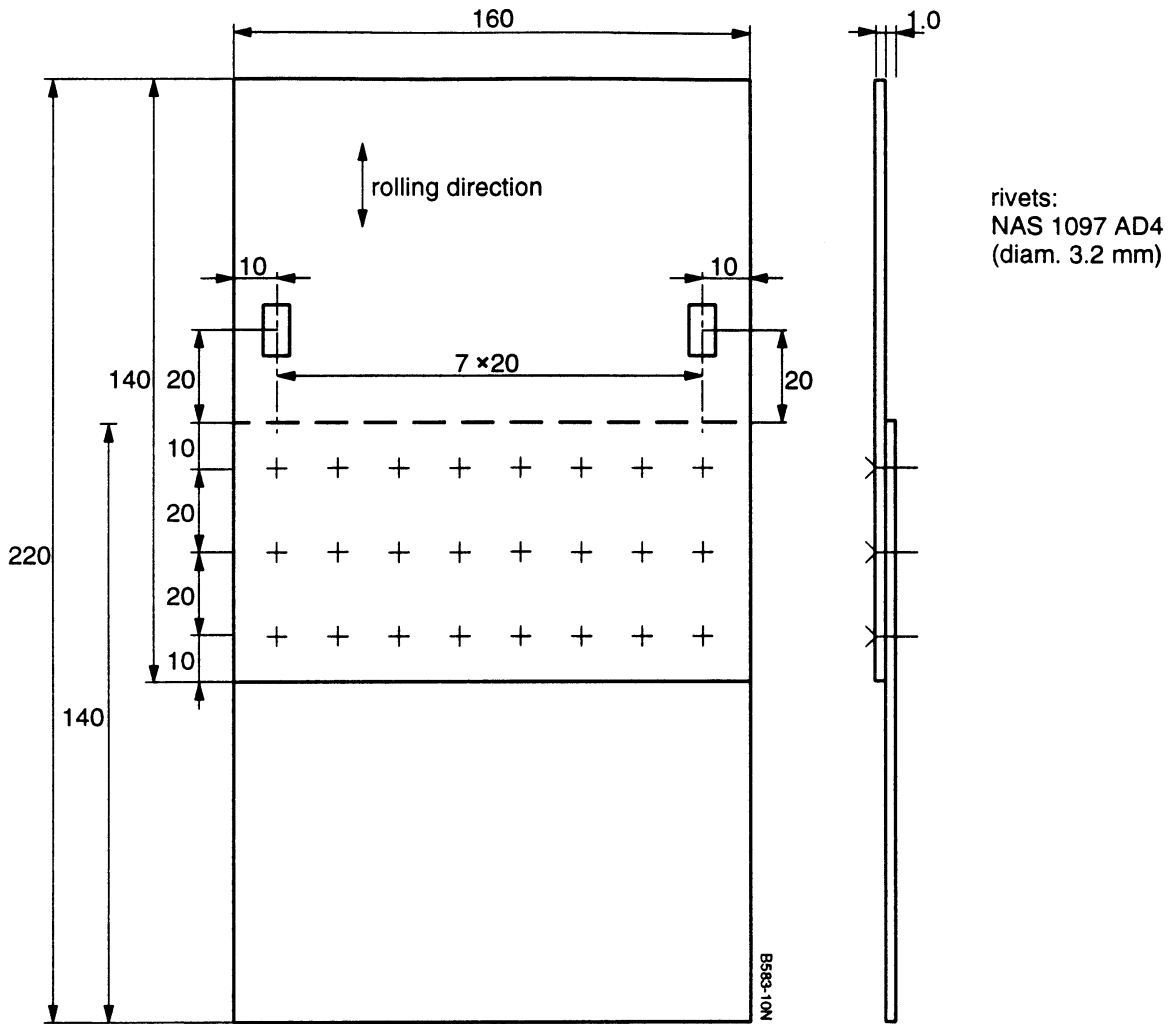


**clamping arms:**

1. Consisting of unidirectional Aramid fibers embedded in epoxy resin in lap joint direction and glass fibers only normal to lap joint (for 480-mm-wide specimens, see text)
2. Cold bonded to specimen and end fixtures with Agomet F310 (Permacol)

**FIGURE 6. EXPLODED VIEW OF 160-mm-WIDE BIAXIAL LAP JOINT SPECIMEN (HALF SPECIMEN DRAWN)**

To check the correct alignment of the specimens during testing to obtain a symmetrical stress distribution across the specimen width, all specimens were provided with two (end load) strain gauges, i.e., one on the left-hand side and one on the right-hand side. The positions of these gauges are given in figure 7. The type of gauges used was HBM 3/120 LY63.



Note: All dimensions are in mm

FIGURE 7. POSITION OF STRAIN GAUGES ON 160-mm-WIDE LAP JOINT SPECIMENS

During the tests, all rivet rows (at either side) were inspected using a travelling microscope combined with a crack monitoring device (Sony Magnecsale EA-210). When a crack was found, the crack length was measured by positioning the crosshairs of the microscope at the extremities of the crack (i.e., at the rivet head edge and at the crack tip). The inspection frequency used during the testing program was based on initiation lives experience obtained from the tests.

Initially inspections were carried out at rather small inspection intervals (every 10,000 cycles) but these intervals increased as more experience was obtained on crack initiation lives. After crack

initiation was detected in a certain test, the inspections were carried out with smaller intervals to collect as much crack propagation data as possible.

#### 4.2 BIAXIAL TESTS.

The biaxial, constant amplitude fatigue tests were carried out in a biaxial fatigue testing frame containing two double-acting hydraulic actuators (see figure 8a). The actuators had a maximum capacity of 200 kN (horizontal actuator) and 100 kN (vertical actuator) and were controlled by closed-loop servo systems. Double-bridge load cells were mounted at the rod ends of the actuators. The load systems of the test frame were controlled by a computerized signal generator and control system.

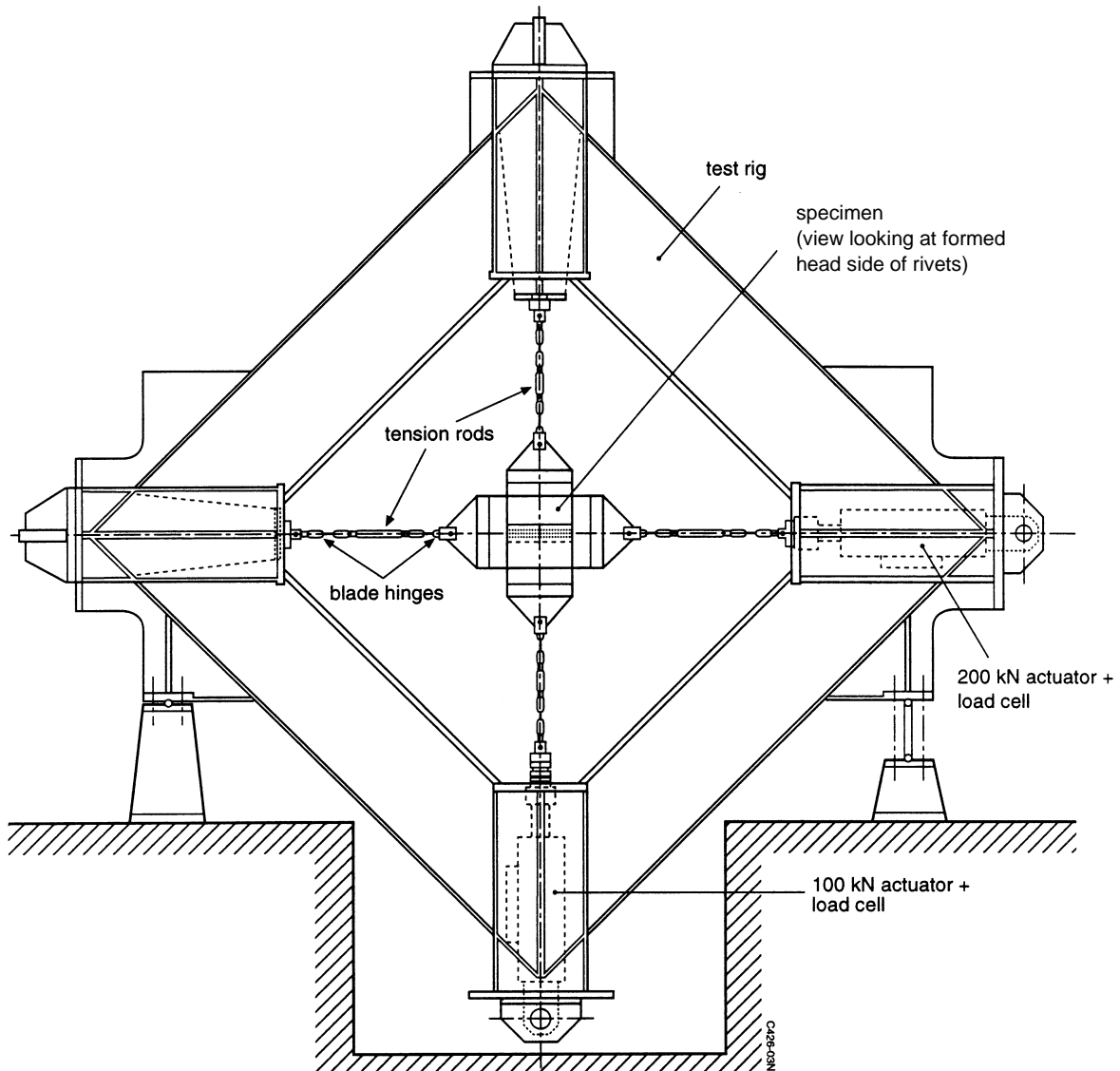


FIGURE 8a. BIAXIAL TEST SETUP

Like the uniaxial tests, the maximum stress level in a cycle (normal to the lap joint) was 94 MPa nominal. The actual applied stress levels and the resulting specimen end loads are given in table 2.

A chart range of 50 kN was used. All specimens were subjected to in-phase biaxial stresses representing the fuselage pressurization stress cycles with a biaxiality ratio (ratio of longitudinal-to-hoop stress) of 0.5. The synchronization of the phases of both load systems was controlled by the software of the control system.

During the tests, the ends of the four arms of the cruciform specimens were bolted to triangular plate fixtures which were connected to adjustable tension rods (see figure 8a). For each load system, one of these tension rods was connected to the actuator load cell and the other to the structure of the test frame. At their ends, the tension rods were provided with blade hinges. Figure 8b shows one of the biaxial specimens mounted in the test frame.

All tests were carried out under load control with an R-ratio of 0.1 and a frequency of 3 Hz. At that frequency no dynamic effects were experienced so that no special fixturing was required.

Similar to the way described in section 4.1 for the uniaxial tests, the specimens were aligned in the test frame during testing using strain gauges, but now a total of eight strain gauges were used, i.e., four for each load direction. The positions of the strain gauges on the specimens are shown in figure 8c. The strain gauges of each load system were connected in a Wheatstone bridge.

The alignment of the specimen in the test frame was carried out as follows.

First, a static alignment was performed by adjusting the lengths of the tension rods in such a way that the panel center was at the center of the test frame. Then, preloads of 1.33 times the maximum test loads occurring in a cycle were applied to the specimen in both directions. Finally, the alignment was further fine-tuned dynamically (starting at a low test frequency) by balancing the output of the Wheatstone bridges of both loading systems (see figure 8c).

The inspections during the tests were carried out in a similar way as described for the uniaxial tests with the exception that no travelling microscope combined with a crack monitoring device was available at the biaxial test frame. Instead, the inspections were performed using a magnifying glass and a torch. To determine the moment and the locations of crack initiation, the visual inspections were supported by means of high-frequency eddy-current inspections using the calibration specimens that were manufactured particularly for that purpose (see last paragraph of section 2).

TABLE 2. SUMMARY OF APPLIED LOADS

specimen no.	width (mm)	thickness (mm)	vertically				horizontally				
			$F_{max}$ (N)	$F_{min}$ (N)	$\sigma_{max}$ (MPa)	$\Delta\sigma$ (MPa)	b (mm)	$F_{max}$ (N)	$F_{min}$ (N)	$\sigma_{max}$ (MPa)	$\Delta\sigma$ (MPa)
C4c	119.9	1.01	11504	1150.4	95.0	85.5	280	13423	1342	47.9	43.2
C5c	120	1.0	11506	1151	95.9	86.3					
C4d	119.9	1.01	11504	1150.4	95.0	85.5					
C5d	120	1.0	11506	1151	95.9	86.3					
C4e	119.8	1.01	11494.8	1149.48	95.0	85.5					
C5e	120	1.0	11506	1151	95.9	86.3					
C4f	120	1.01	11541	1154.1	95.2	85.7					
C5f	120	1.0	11506	1151	95.9	86.3					
C1c	160	1.0	15416	1542	96.4	86.7					
C2c	160.1	1.01	15362	1536.2	95	85.5					
C3c	160	1.0	15200	1520	95	85.5					
C1e	160.15	1.01	15366	1536.6	95	85.5					
C2e	160	1.01	15352	1535.2	95	85.5					
C3e	160	1.0	15416	1542	96.4	86.7					
								13160	1316	47.0	42.3
								13160	1316	47.0	42.3

specimen no.	width (mm)	thickness (mm)	vertically				horizontally				
			$F_{max}$ (kN)	$F_{min}$ (kN)	$\sigma_{max}$ (MPa)	$\Delta\sigma$ (MPa)	length (mm)	$F_{max}$ (kN)	$F_{min}$ (kN)	$\sigma_{max}$ (MPa)	$\Delta\sigma$ (MPa)
C1a	480	1.0	45.12	4.512	94	84.6	280	13.16	1.316	47	42.3
C2a											
C3a											
C4a											
C5a											
C6a											
D3a	480	1.0	45.12	4.512	94	84.6	220	11.75	1.175	47	42.3
D4a											
D5a											

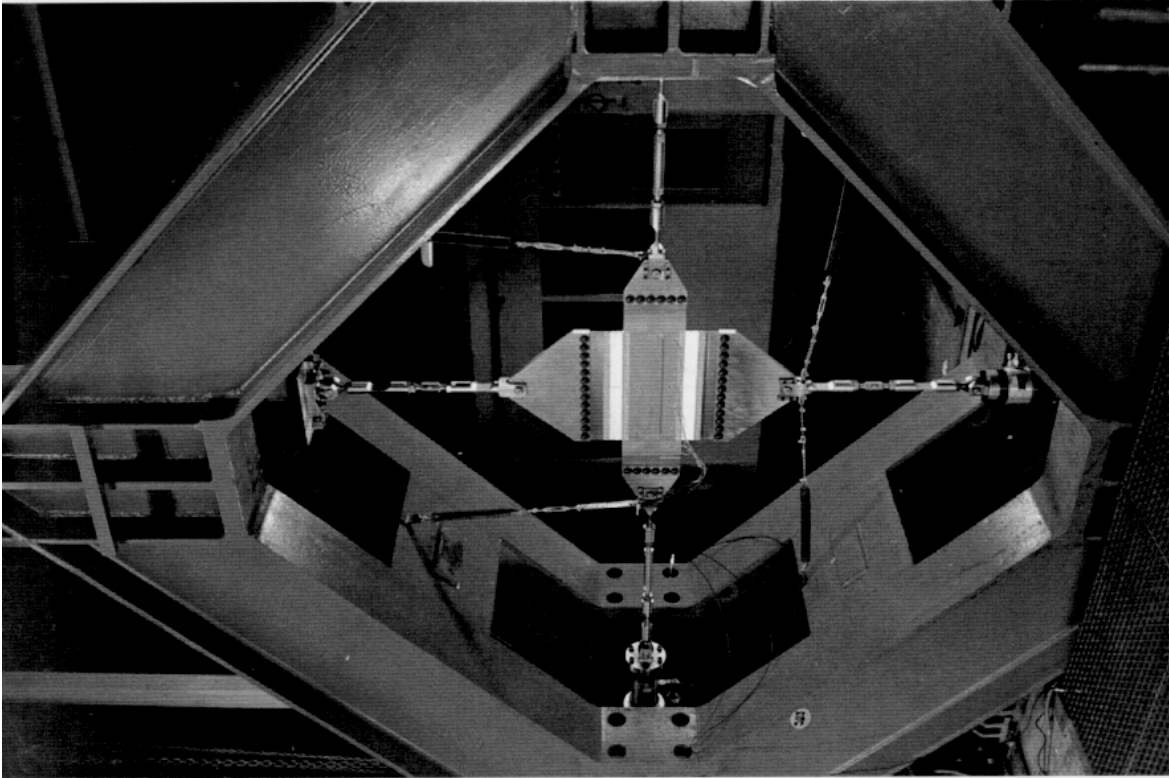
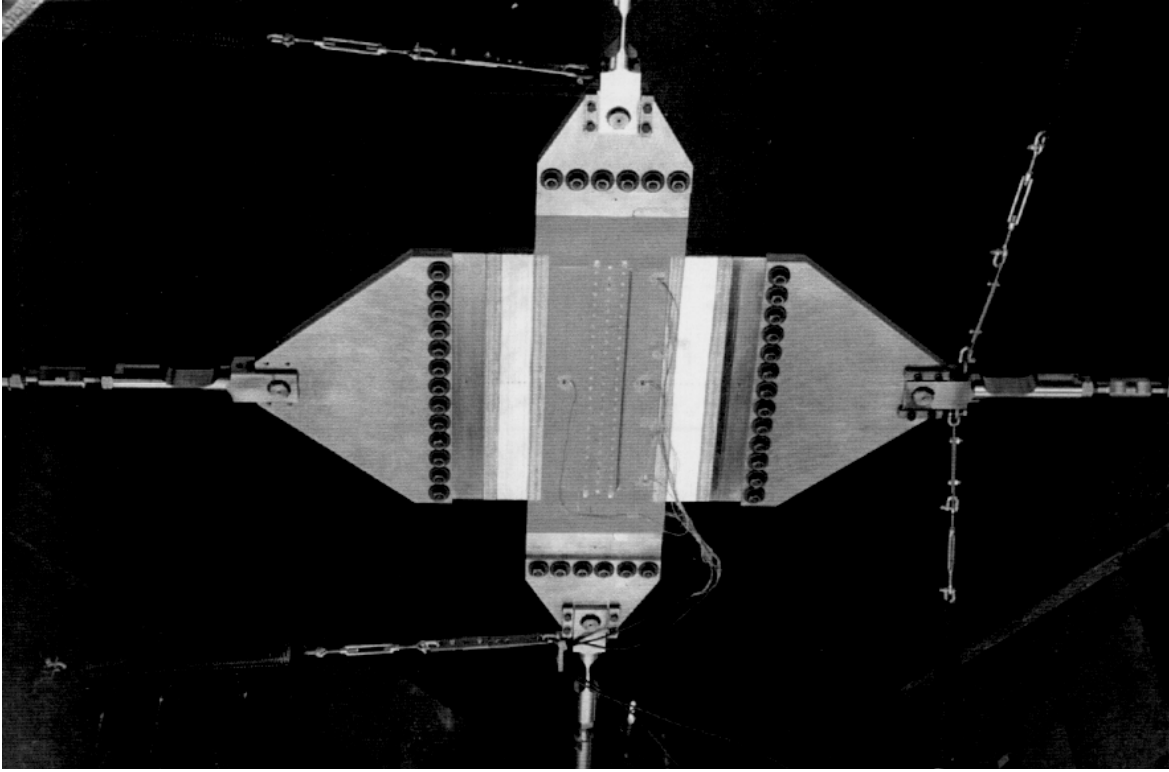
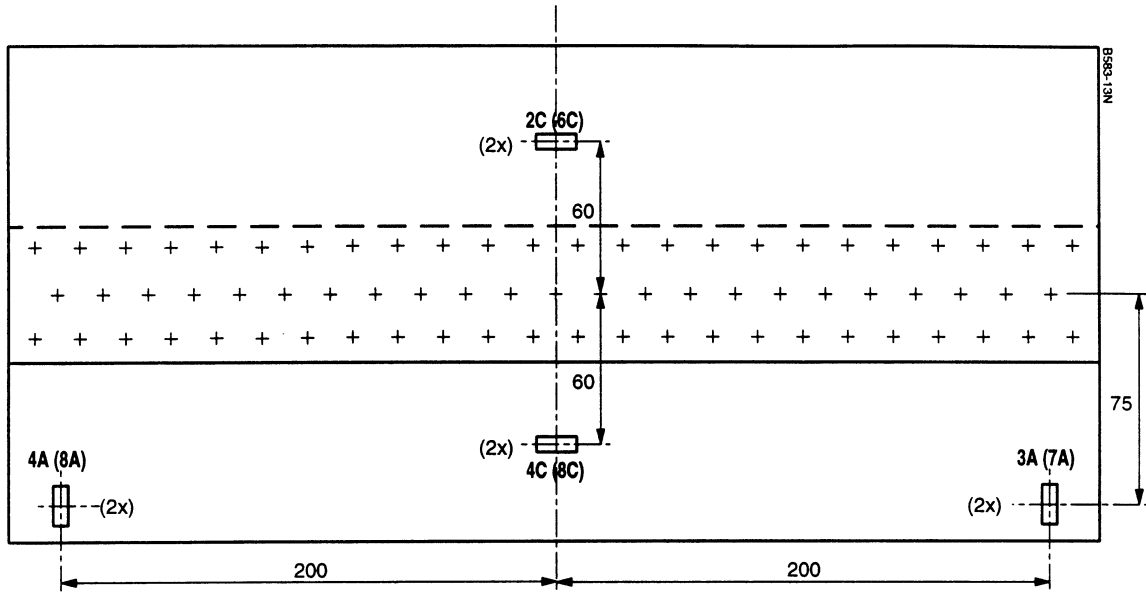


FIGURE 8b. ONE OF THE 480-mm-WIDE BIAXIAL SPECIMENS MOUNTED IN THE TEST FRAME



Note: All dimensions are in mm

**Connection of strain gauges in Wheatstone bridges**

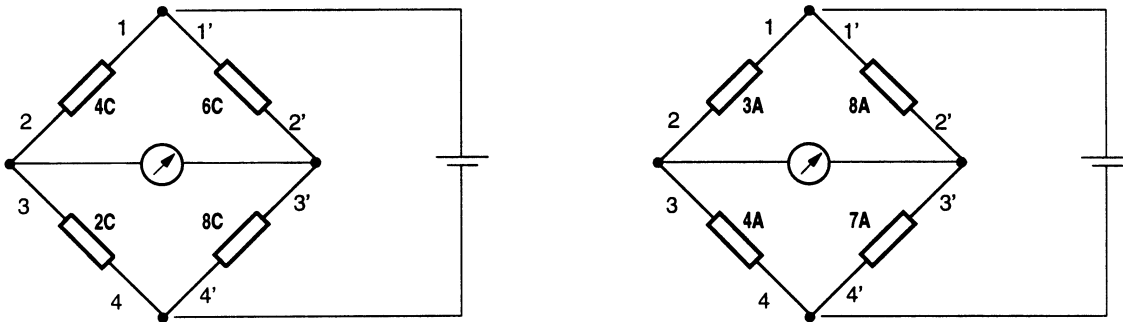


FIGURE 8c. POSITIONS OF STRAIN GUAGES ON SPECIMEN TO REALIZE A CORRECT ALIGNMENT DURING THE TEST

5. SPATE MEASUREMENT PERFORMED.

The stress distribution in panel D4a was investigated by means of thermo-elastic equipment (SPATE 8000). SPATE measures the sum of the principal stresses.

6. RESULTS OF TESTS AND MEASUREMENTS.

Table 3 summarizes a survey of the uniaxial and biaxial fatigue test results and shows the number of kilocycles at which the first cracks initiated and the number of kilocycles at which the specimen failed. The test results will be discussed in more detail in the following section.

TABLE 3. SUMMARY OF THE TEST RESULTS

Countersunk specimens, fully bonded

Specimen No.	Specimen Width (mm)	Uniaxial/Biaxial	First Crack (kilocycles)	First Linkup (kilocycles)	Failure (kilocycles)
C1c	160	biaxial	—	—	500 *
C2c	160	uniaxial	—	—	500 *
C3c	160	uniaxial	—	—	500 *
C4c	120	uniaxial	—	—	500 *
C5c	120	biaxial	—	—	1000 *
C2a	480	biaxial	—	—	1000 *

Countersunk specimens, partly bonded

Specimen No.	Specimen Width (mm)	Uniaxial/Biaxial	First Crack (kilocycles)	First Linkup (kilocycles)	Failure (kilocycles)
C4d	120	uniaxial	—	—	500 *
C5d	120	biaxial	—	—	500 *

Countersunk specimens, degradation of bonding

Specimen No.	Specimen Width (mm)	Uniaxial/Biaxial	First Crack (kilocycles)	First Linkup (kilocycles)	Failure (kilocycles)
C1e	160	uniaxial	275	311	311
C2e	160	uniaxial	200	201	202
C3e	160	biaxial	250	397	303
C4e	120	uniaxial	175	218	218
C5e	120	biaxial	313	355	357
C1a	480	biaxial	225	303	307
C3a	480	biaxial	—	—	1000 *

Countersunk specimens, fully unbonded

Specimen No.	Specimen Width (mm)	Uniaxial/Biaxial	First Crack (kilocycles)	First Linkup (kilocycles)	Failure (kilocycles)
C4f	120	uniaxial	150	182	182
C5f	120	biaxial	213	263	263
C4a	480	biaxial	460	548	557
C5a	480	biaxial	588	600	605
C6a	480	biaxial	434	434	438

Dimpled specimens, fully unbonded

Specimen No.	Specimen Width (mm)	Uniaxial/Biaxial	First Crack (kilocycles)	First Linkup (kilocycles)	Failure (kilocycles)
D3a	480	biaxial	120	148	153
D4a	480	biaxial	112	135	137
D5a	480	biaxial	112	124	127

\* Test stopped, no cracks found

In table 4 the measured diameter of the formed heads of the rivets in the critical row are given. These data are only given for the failed specimens.

TABLE 4. DIAMETER (mm) OF THE RIVET FORMED HEAD FOR THE RIVETS IN THE CRITICAL ROW

Specimen	C1e	C2e	C3e			
rivet number						
17	4.91	4.81	—			
18	4.92	4.80	5.21			
19	4.85	4.84	5.11			
20	4.92	4.84	5.14			
21	4.82	5.09	5.08			
22	4.99	4.94	5.14			
23	4.85	4.68	5.24			
24	4.78	4.75	—			
average	4.88	4.84	5.15			
Specimen	C4e	C5e	C5f			
rivet number						
13	4.56	—	—			
14	4.86	4.77	4.80			
15	4.79	5.01	4.77			
16	4.94	4.87	4.72			
17	4.61	4.82	4.42			
18	4.82	—	—			
average	4.76	4.87	4.68			
Specimen	C1a	C2a	C3a	C4a	C5a	C6a
rivet number						
1	—	—	—	—	—	—
2	4.86	5.05	4.91	5.20	5.53	5.20
3	5.08	5.04	4.74	5.11	5.42	5.11
4	5.08	5.08	4.90	4.98	5.08	4.99
5	4.94	4.98	4.86	4.91	5.47	4.92
6	4.96	5.30	4.96	4.85	5.27	4.86
7	4.89	4.90	4.95	4.72	5.02	4.71
8	5.15	5.00	4.98	5.07	5.13	5.07
9	5.08	5.05	4.76	4.97	5.15	4.96
10	5.22	5.09	4.88	4.74	5.36	4.74
11	4.76	5.15	4.95	4.82	5.08	4.82
12	5.21	5.03	4.84	4.88	5.19	4.88
13	4.86	5.13	4.80	4.89	5.08	4.71
14	4.84	4.87	4.94	4.77	5.14	4.78
15	4.99	5.09	4.87	4.94	5.02	4.93
16	5.04	5.15	4.93	4.85	4.91	4.85
17	4.75	4.98	5.00	4.87	5.37	4.87
18	4.63	5.26	5.01	4.92	5.23	4.92
19	5.14	5.04	5.21	5.10	5.14	5.10
20	5.07	5.04	5.12	4.89	4.86	4.88
21	4.66	5.06	5.03	4.78	5.42	4.78
22	4.81	4.88	4.89	5.10	5.04	5.10
23	4.73	5.10	5.10	5.08	4.98	5.08
24	—	—	—	—	—	—
average	4.94	5.06	4.94	4.93	5.18	4.92

Figures 9 to 31 present the test results of each specimen. In these figures the specimen configuration and the applied loading are given. For those specimens with cracks, the crack initiation and the crack growth are given as a function of the number of applied loading cycles. After the failure of the specimen, the fracture surfaces were studied using a binocular. For each failed specimen, a sketch of the fracture surface was made indicating the locations of crack initiation and the extensions of the fatigue cracks up to failure. The results of the SPATE measurements are presented in figure 32.

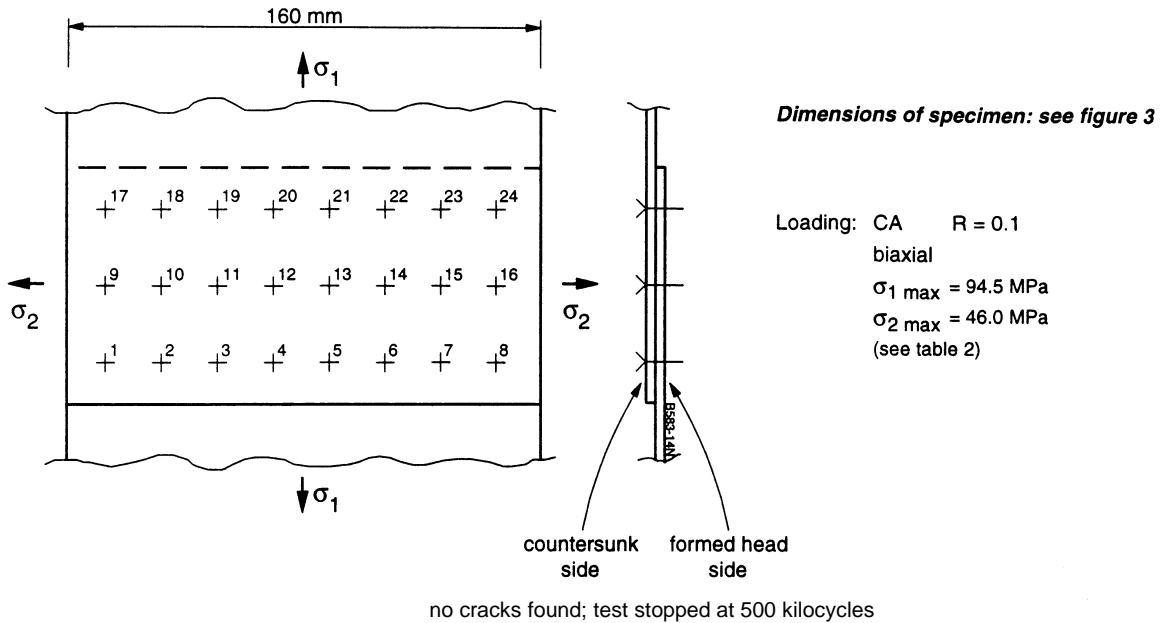


FIGURE 9. RESULTS FOR SPECIMEN C1c

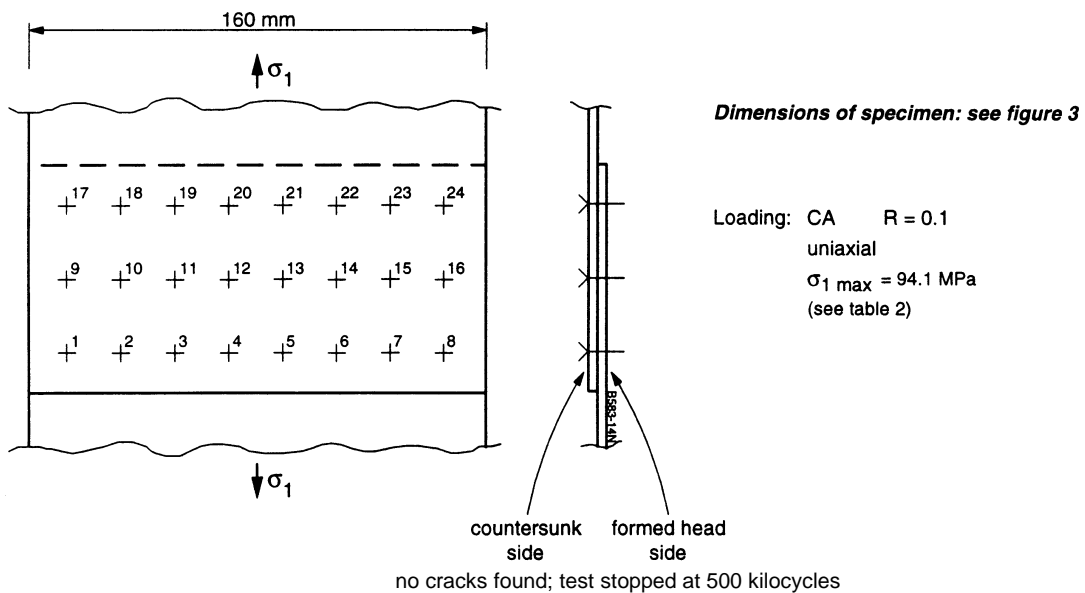


FIGURE 10. RESULTS FOR SPECIMEN C2c

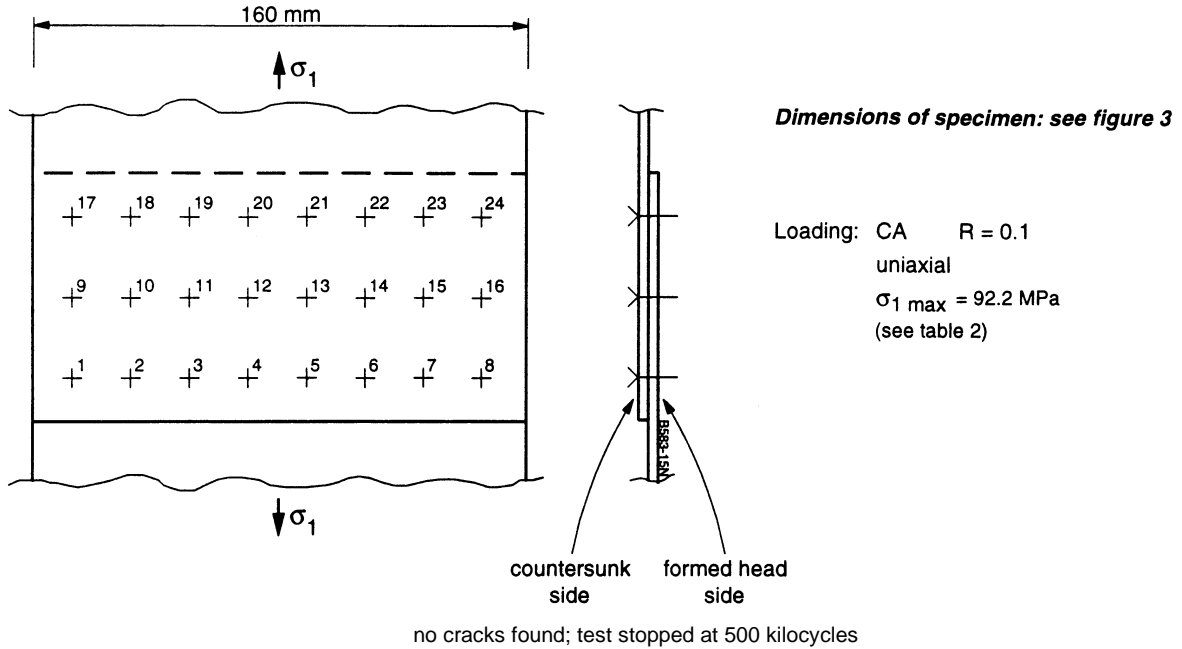


FIGURE 11. RESULTS FOR SPECIMEN C3c

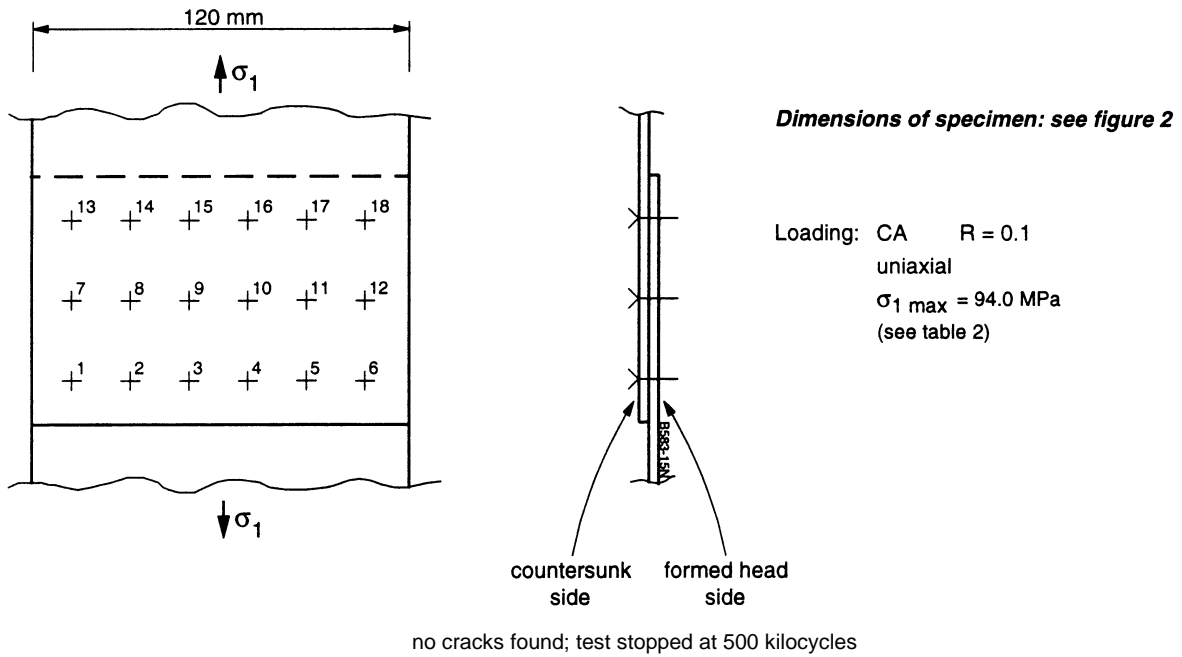


FIGURE 12. RESULTS FOR SPECIMEN C4c

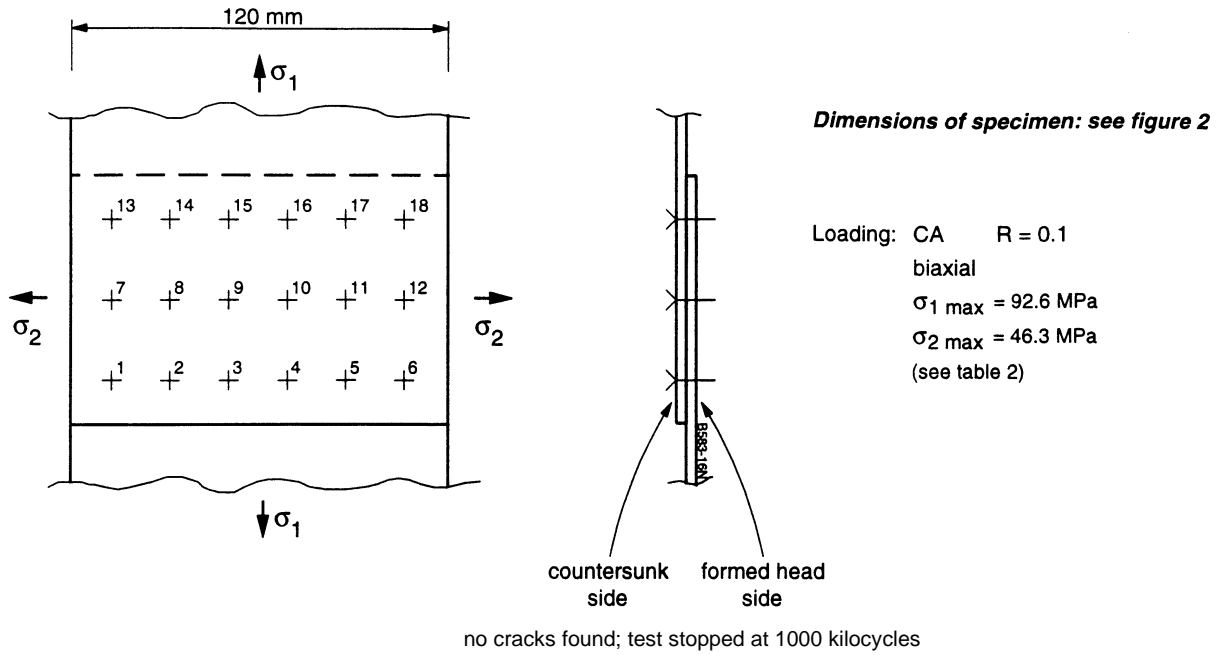


FIGURE 13. RESULTS FOR SPECIMEN C5c

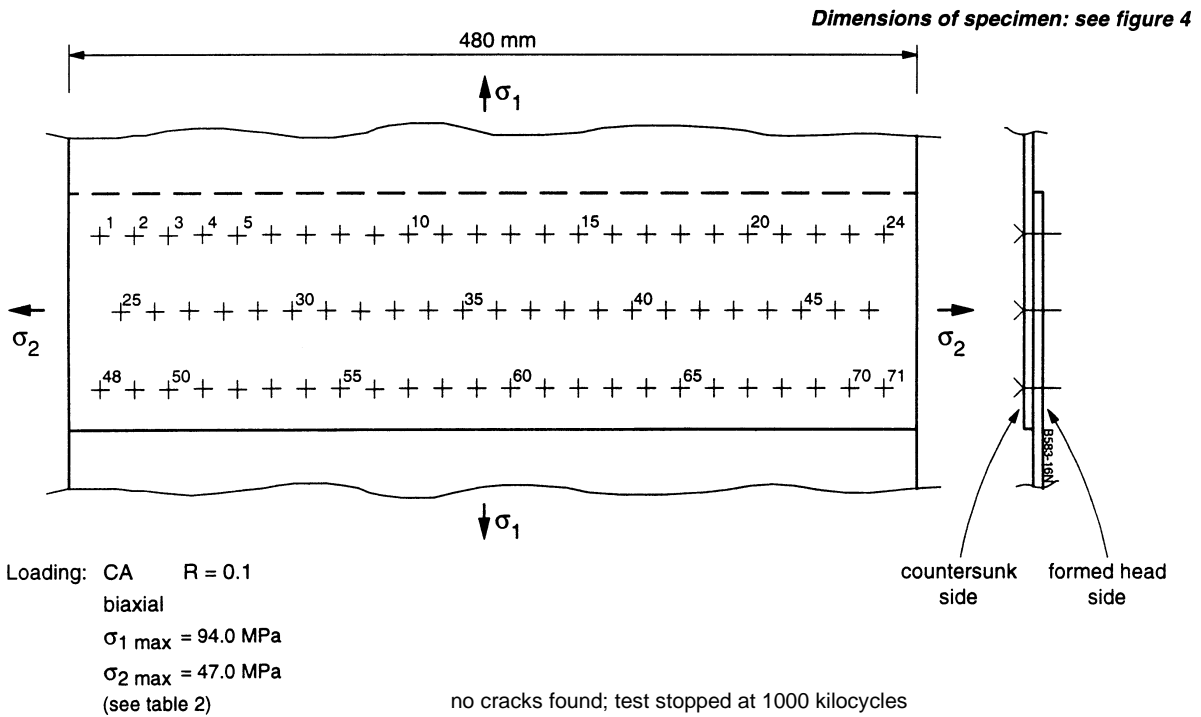


FIGURE 14. RESULTS FOR SPECIMEN C2a

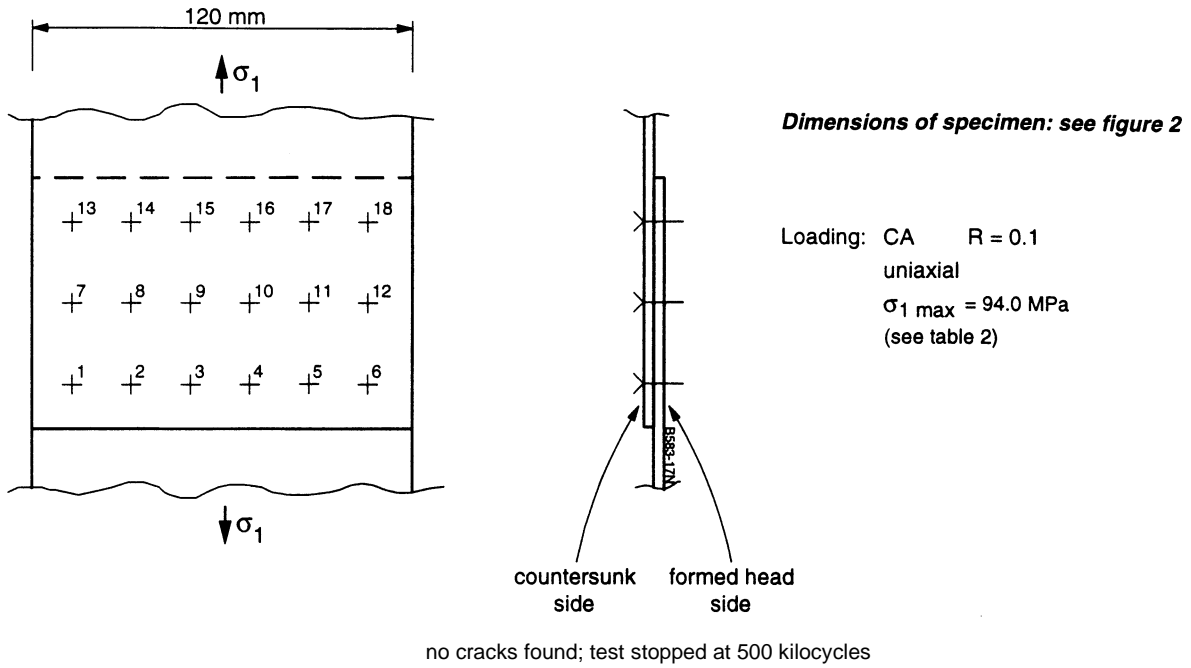


FIGURE 15. RESULTS FOR SPECIMEN C4d

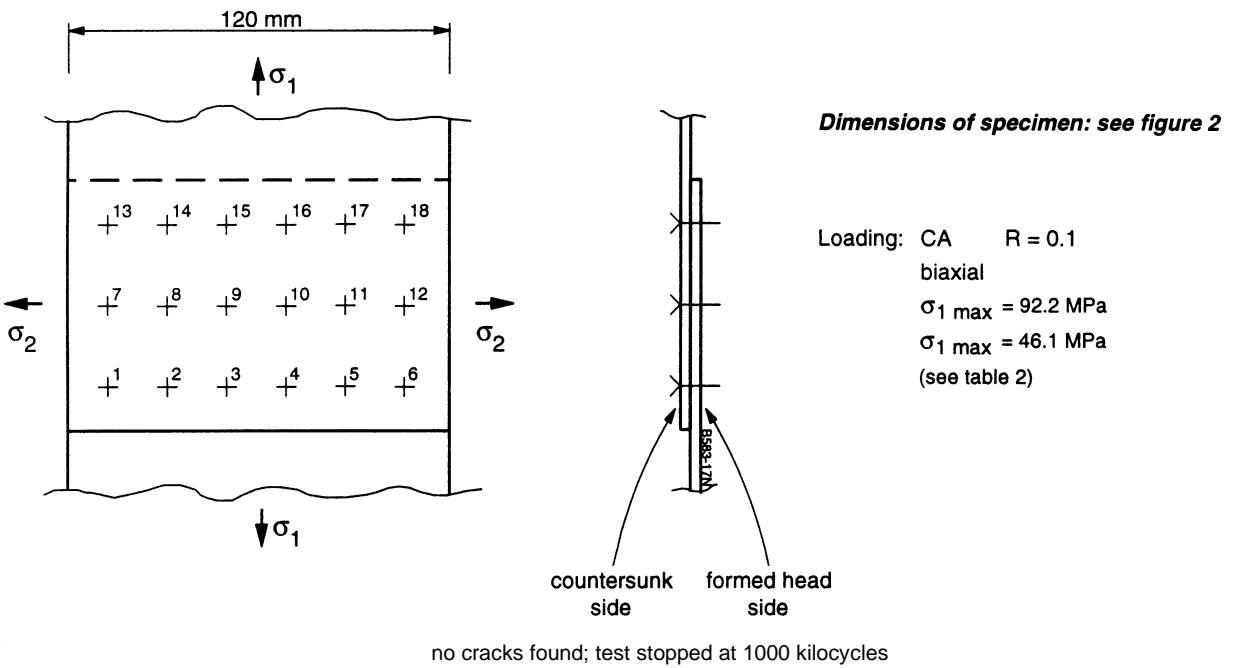
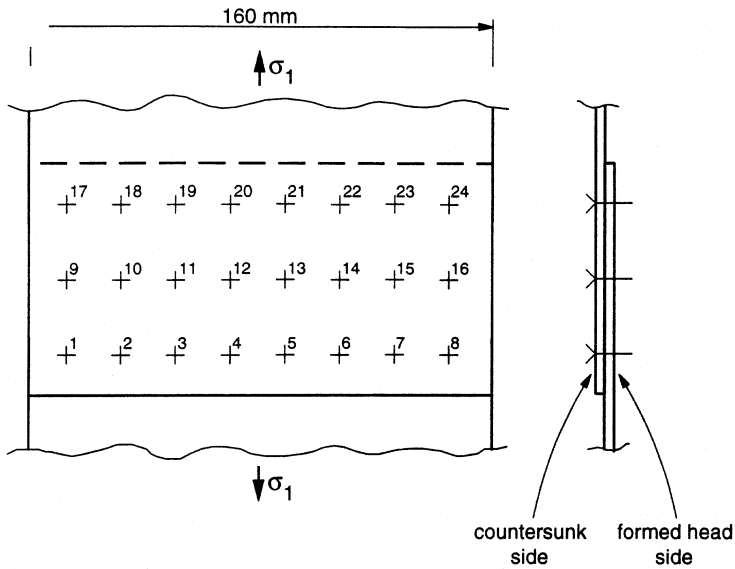


FIGURE 16. RESULTS FOR SPECIMEN C5d



Dimensions of specimen: see figure 3

Loading: CA R = 0.1  
 uniaxial  
 $\sigma_1 \text{ max} = 94.2 \text{ MPa}$   
 (see table 2)

● crack initiation  
 ↑ crack position

		countersunk side											
cycles (10 <sup>3</sup> )	18		19		20		21		22		23		
	L	R	L	R	L	R	L	R	L	R	L	R	
275	1.0	○			4.0	○							
280	1.4	○			4.5	○	1.2						
285	1.7	○			4.8	○	1.6						
290	2.3	○			5.5	○	2.3						
295	2.5	○			6.2	○	2.8						
300	3.3	○			7.0	○	4.0						
305	4.0	○	1.5	○	1.5	○	8.0	○	4.5				
310	4.8	○	1.5	○	4.5	○	4.8	11.5	○	7.6	2.0	○	
311.32	FAILURE												

Note: All crack lengths are in mm

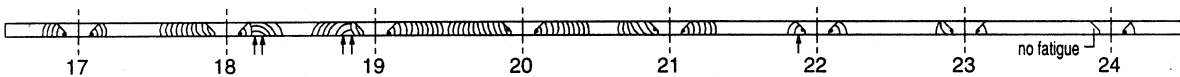
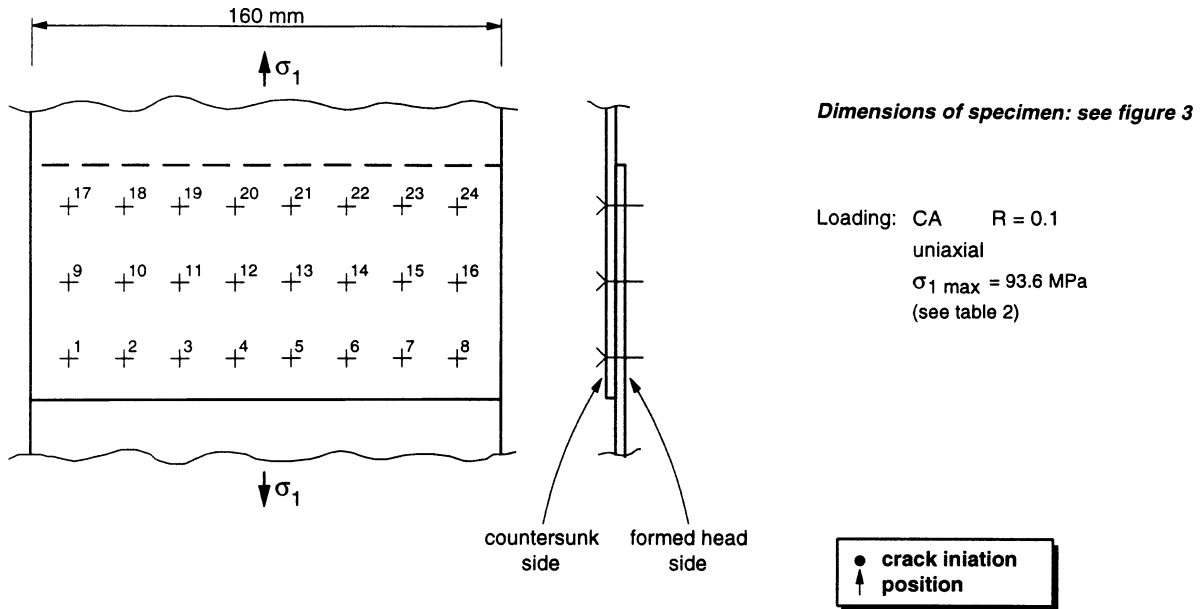


FIGURE 17. RESULTS FOR SPECIMEN C1e



		countersunk side											
cycles ( $10^3$ )	18		19		20		21		22		23		
	L	R	L	R	L	R	L	R	L	R	L	R	
50													
100													
150													
200							0.5	1.5	10.0	10.5	5.6	2.7	
201							2.8			11.5	6.5	5.2	
202			1.0		1.1	0.8	6.0			12.2	7.2	10.0	
202.20	FAILURE												

Note: All crack lengths are in mm

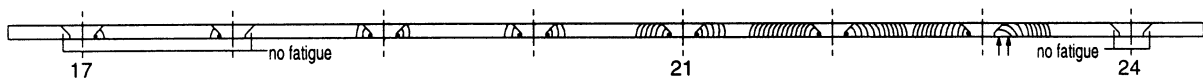
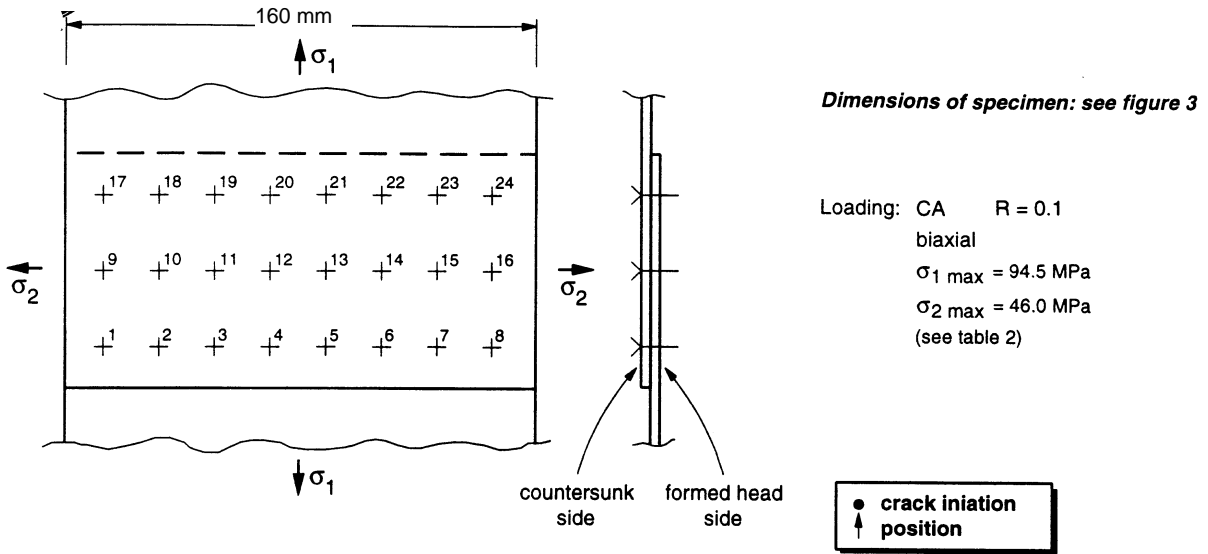


FIGURE 18. RESULTS FOR SPECIMEN C2e



cycles (10 <sup>3</sup> )	countersunk side											
	18		19		20		21		22		23	
	L	R	L	R	L	R	L	R	L	R	L	R
250					2	○						
255					2.8	○						
261					3.5	○	1.5					
265.5			1	○	4.5	○	2.8					
270			2	○	5	○	3.5					
275.5			3	○	5.5	○	4					
280			3.5	○	6	○	4.5					
286			4	○	1	7	○	6				
291.5			5	○	3	9	○	7	1	○		
297			8.5	○	6	12	○	3	○			
300			11.5	○	6	13	○	8	○			
301			12.5	○	7	13.5	○	9.5	○			
302			14	○	8.5	14	○	12.5	○	1.5		
302.5			16.5	○	8.5	14.5	○	16	○	3.5		
303	2	○	18	○	8.5	15	○	7	○			
303.4	FAILURE											

Note: All crack lengths are in mm

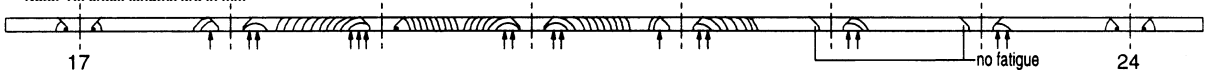
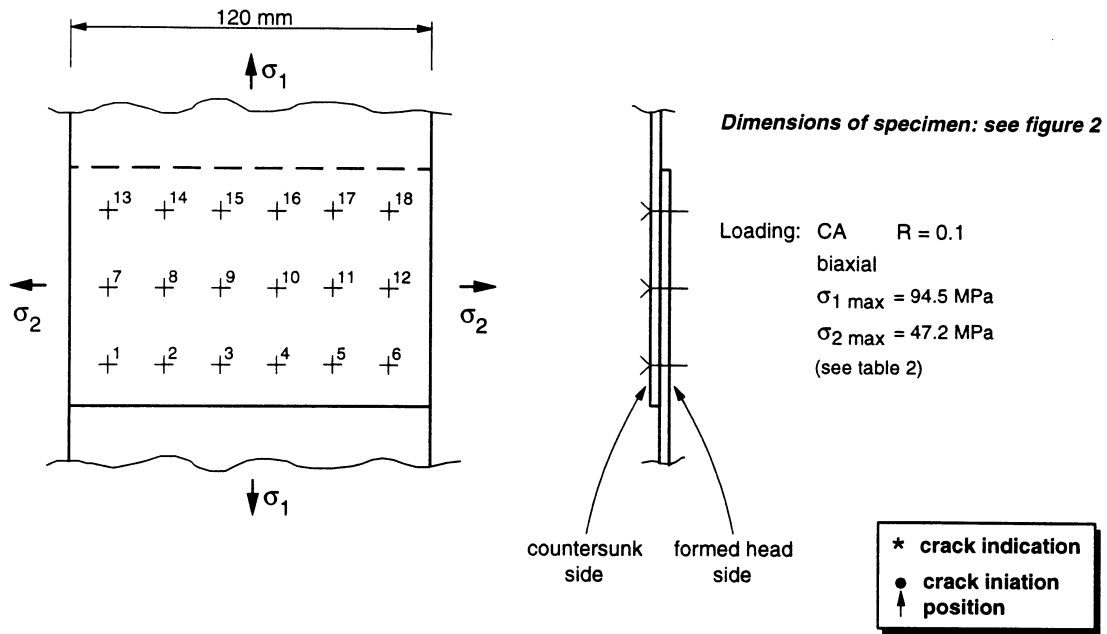


FIGURE 19. RESULTS FOR SPECIMEN C3e





		countersunk side											
cycles (10 <sup>3</sup> )	13		14		15		16		17		18		
	L	R	L	R	L	R	L	R	L	R	L	R	
312.5							* ○ 0.5						
322.5					○ 0.5	○ 0.5	○ 1.0	○ 2.0					
330					○ 1.5	○ 1.5	○ 2.5	○ 3.0					
335					○ 2.0	○ 2.5	○ 2.5	○ 4.0					
340					○ 2.5	○ 3.0	○ 3.5	○ 5.0					
345	○	*	○ 0.5		○ 3.0	○ 3.5	○ 4.0	○ 5.5					
350	○ 1.0		○ 2.0		○ 4.0	○ 4.5	○ 5.0	○ 6.5	* ○ *				
353.75	○ 1.5		○ 2.5		○ 5.0	○ 5.5	○ 6.5	○ 7.5	○ 1.5	○ 1.5			
355	○ 1.5		○ 0.5 3.0		○ 6.0	○ 8.5	○ 8.5	○ 3.0	○ 2.0				
356.25	○ 2.5		○ 1.0 4.0		○ 7.0	○ 9.5	○ 9.5	○ 3.5	○ 3.0				
356.95	FAILURE												

Note: All crack lengths are in mm

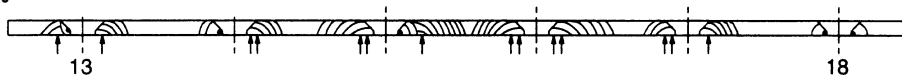
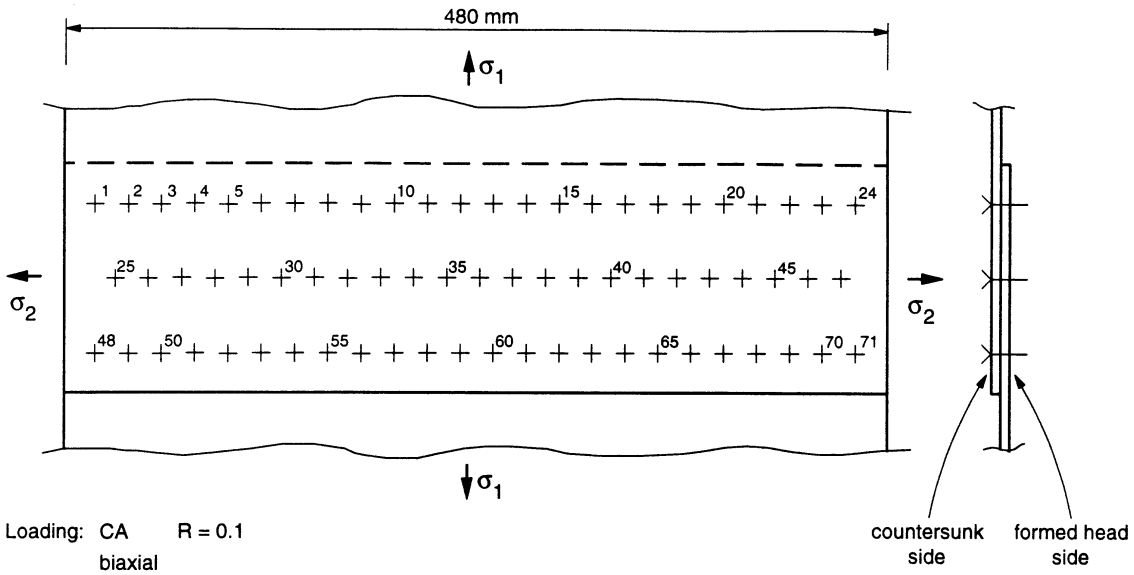


FIGURE 21. RESULTS FOR SPECIMEN C5e

Dimensions of specimen: see figure 4



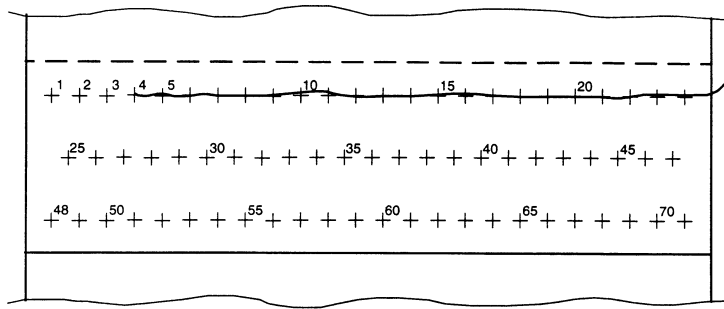
Loading: CA R = 0.1  
 biaxial  
 $\sigma_1 \text{ max} = 94.0 \text{ MPa}$   
 $\sigma_2 \text{ max} = 47.0 \text{ MPa}$   
 (see table 2)

\* crack indication  
 ● crack initiation  
 ↑ position

countersunk side																								
cycles (10 <sup>3</sup> )	1	2	3	4	5	6	7	8	9	10	11	12	13	14	15	16	17	18	19	20	21	22	23	24
	L	R	L	R	L	R	L	R	L	R	L	R	L	R	L	R	L	R	L	R	L	R	L	R
225																								1.0
250																								* 4.5
262.5																							1.5 5.5	
275																					1.0 *		3.0 7.5	
282.5																					2.0 0.5		4.5 9.0	● ball indentation
290																					3.0 0.5		7.0 9.0	
297.5																					3.5 0.5		9.5 9.0	
302.5																					4.5 1.0		9.0	
307.1																								FAILURE

Note: All crack lengths are in mm

FIGURE 22. RESULTS FOR SPECIMEN C1a



Failure mode

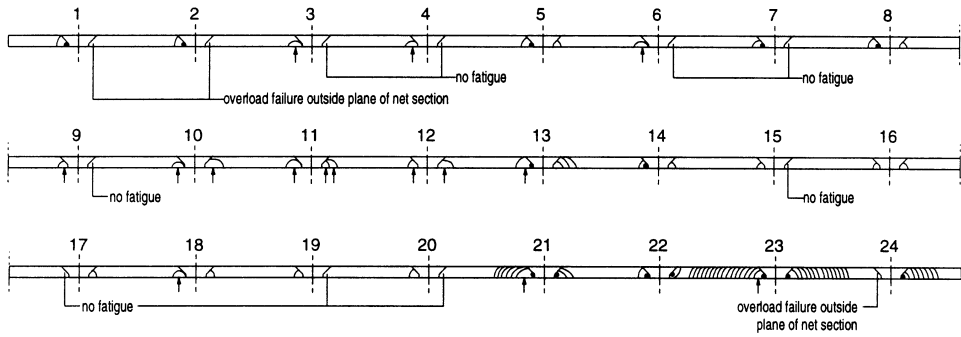


FIGURE 22. RESULTS FOR SPECIMEN C1a (CONTINUED)

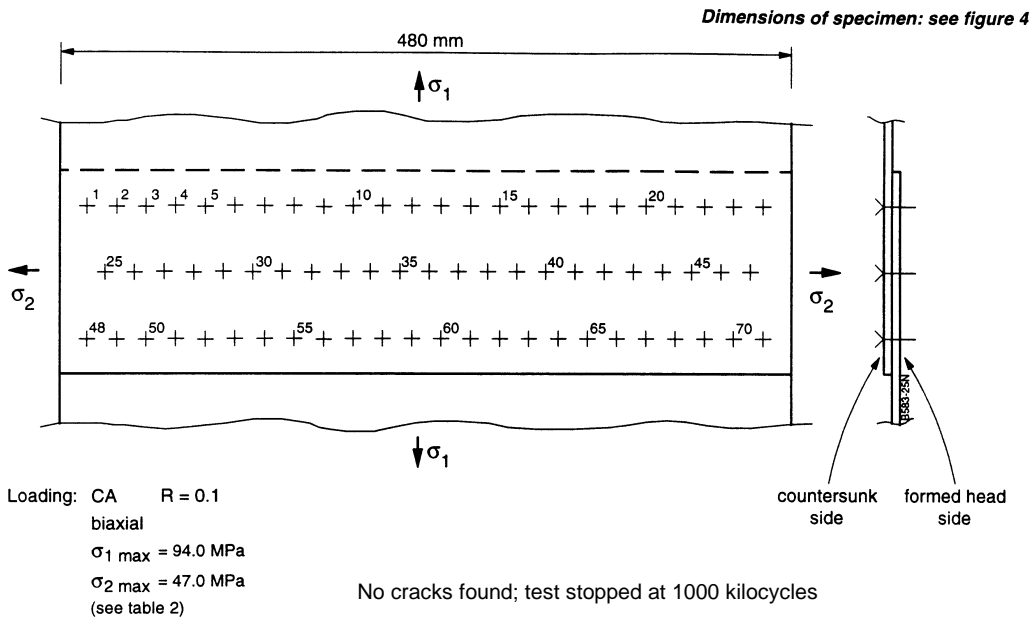
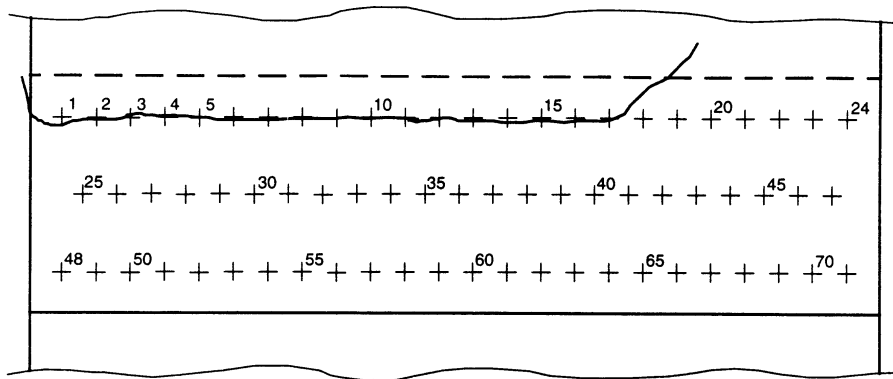


FIGURE 23. RESULTS FOR SPECIMEN C3a









Failure mode

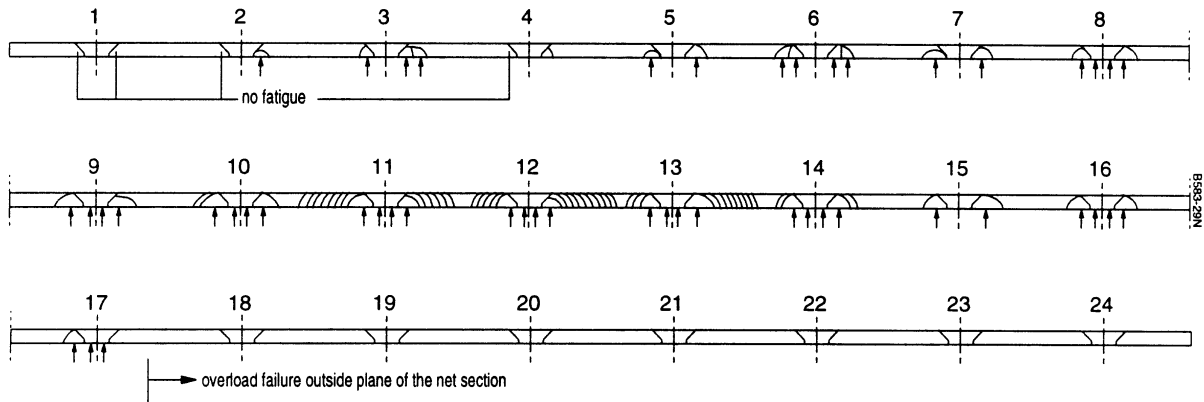
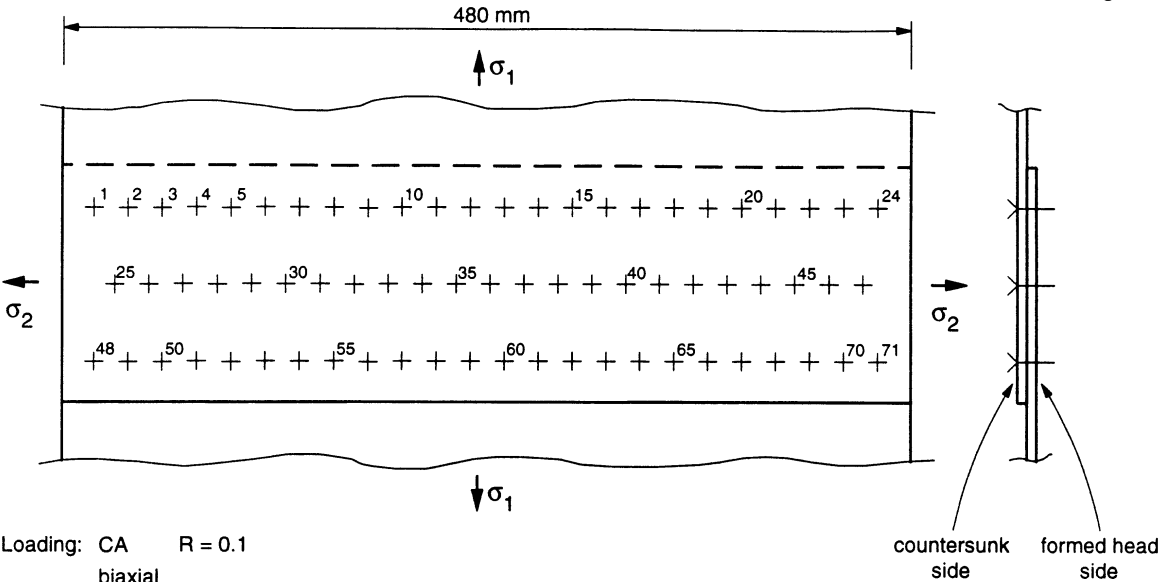


FIGURE 26. RESULTS FOR SPECIMEN C4a (CONTINUED)

Dimensions of specimen: see figure 4



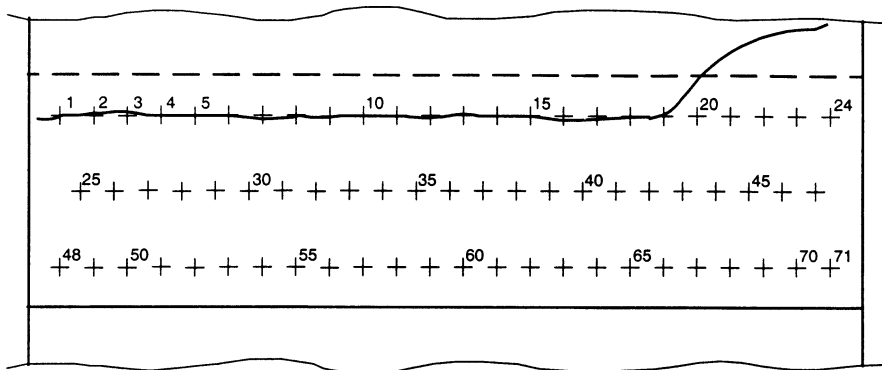
Loading: CA R = 0.1  
 biaxial  
 $\sigma_1 \text{ max} = 94.0 \text{ MPa}$   
 $\sigma_2 \text{ max} = 47.0 \text{ MPa}$   
 (see table 2)

● crack initiation  
 ↑ position

	countersunk side																							
cycles (10 <sup>3</sup> )	1	2	3	4	5	6	7	8	9	10	11	12	13	14	15	16	17	18	19	20	21	22	23	24
587.5	L	R	L	R	L	R	L	R	L	R	L	R	L	R	L	R	L	R	L	R	L	R	L	R
595	1.0	0.5																						
600	10.5	2.0																						
602.5	5.0																							
604.84	16.0																							
			FAILURE																					

Note: All crack lengths are in mm

FIGURE 27. RESULTS FOR SPECIMEN C5a



Failure mode

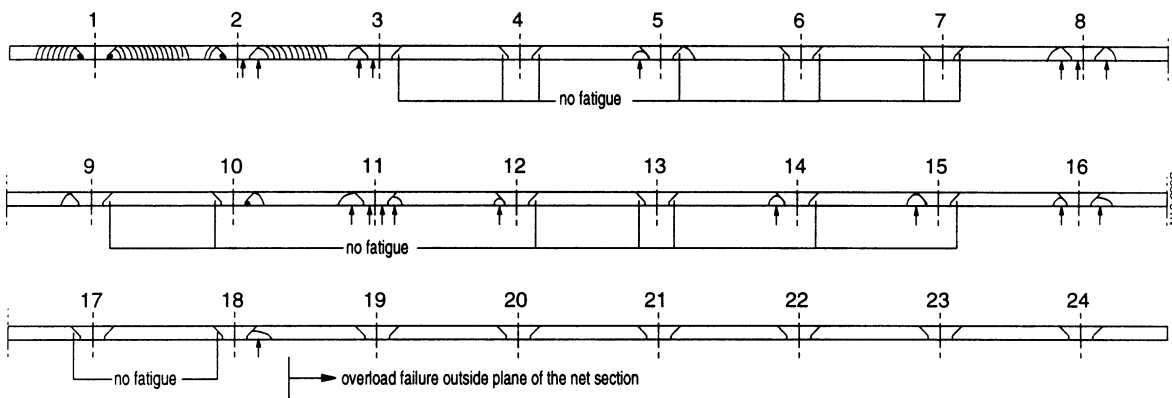
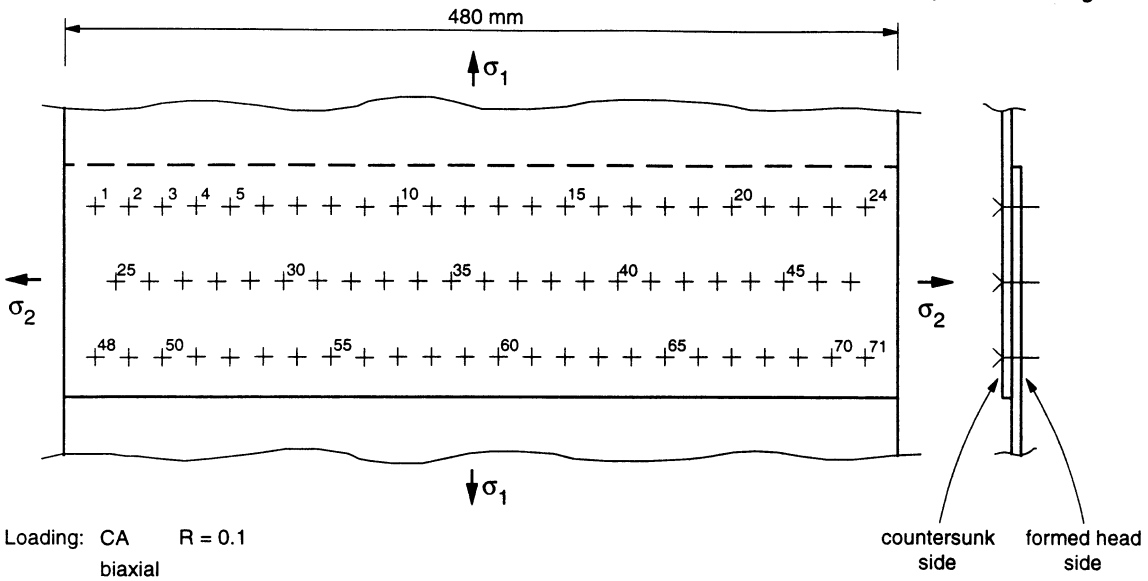


FIGURE 27. RESULTS FOR SPECIMEN C5a (CONTINUED)

Dimensions of specimen: see figure 4

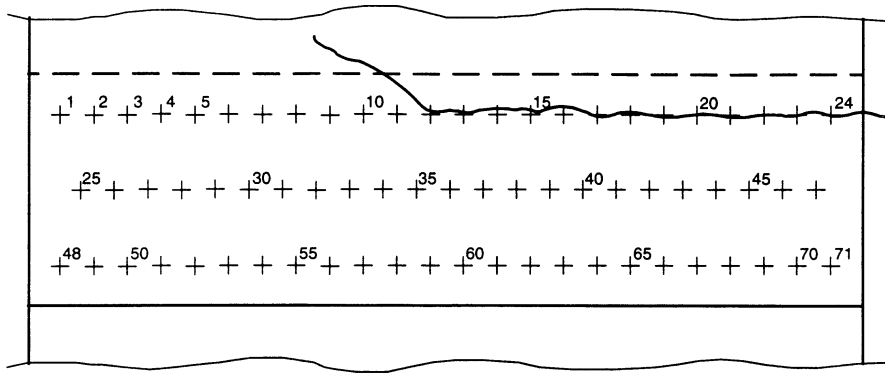


Loading: CA R = 0.1  
 biaxial  
 $\sigma_1 \text{ max} = 94.0 \text{ MPa}$   
 $\sigma_2 \text{ max} = 47.0 \text{ MPa}$

countersunk side																								
cycles (10 <sup>3</sup> )	1	2	3	4	5	6	7	8	9	10	11	12	13	14	15	16	17	18	19	20	21	22	23	24
	L	R	L	R	L	R	L	R	L	R	L	R	L	R	L	R	L	R	L	R	L	R	L	R
434.5																							13.5	
437.5																			19.0					
437.92																								FAILURE

Note: All crack lengths are in mm

FIGURE 28. RESULTS FOR SPECIMEN C6a



Failure mode

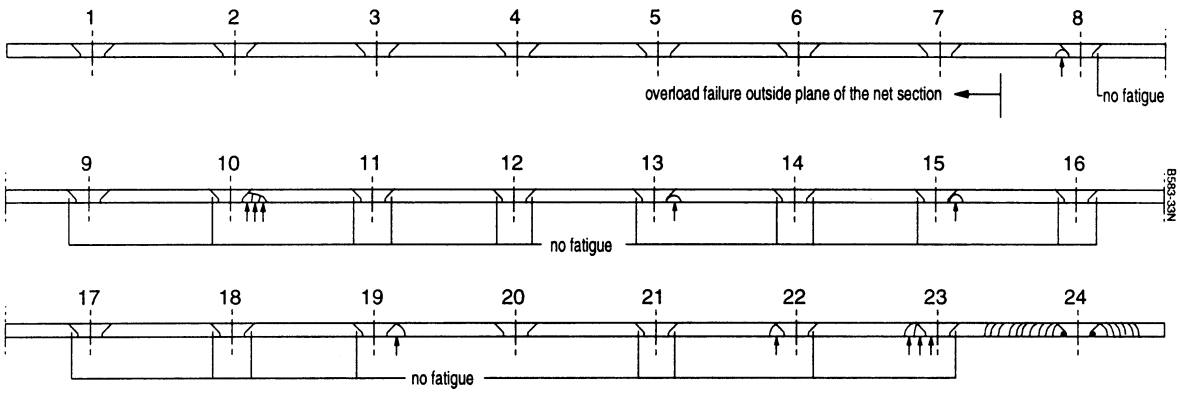
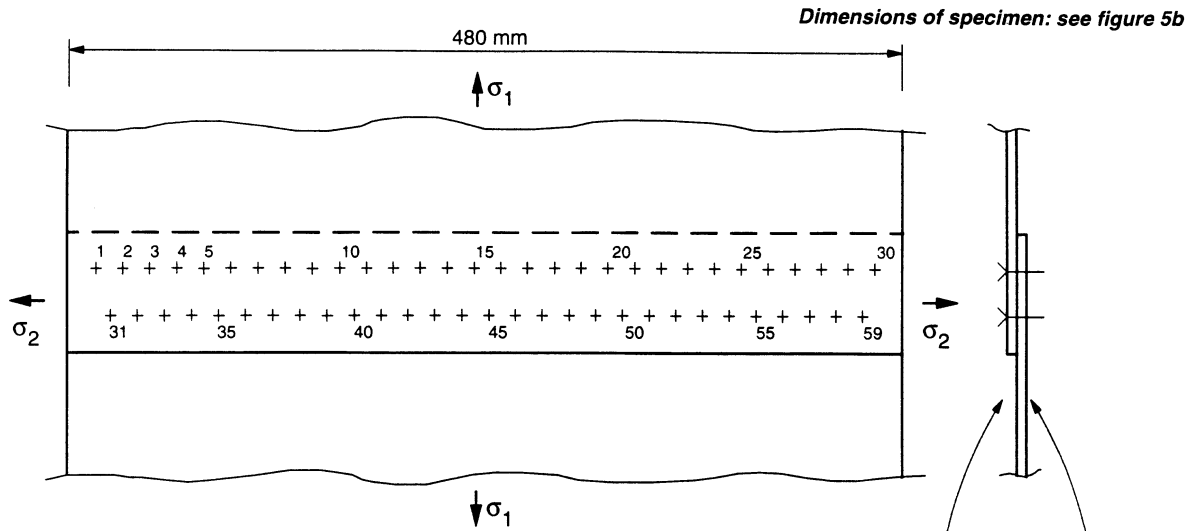


FIGURE 28. RESULTS FOR SPECIMEN C6a (CONTINUED)



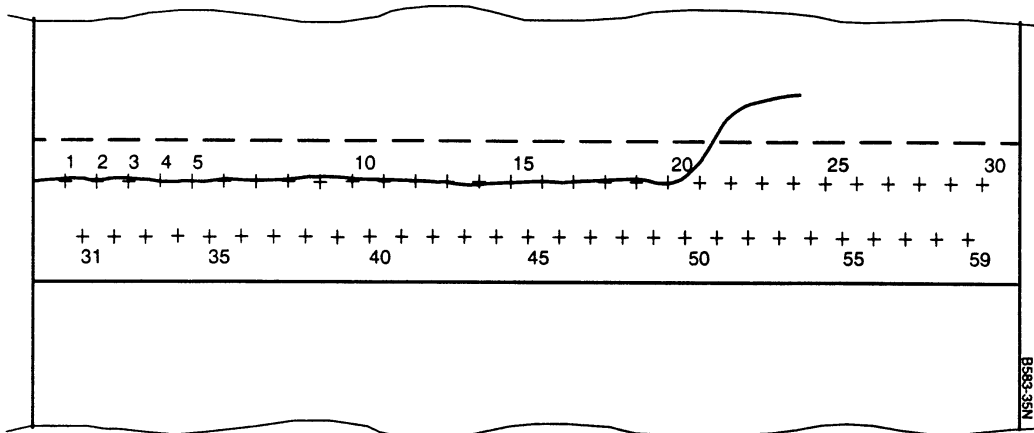
Loading: CA R = 0.1  
 biaxial  
 $\sigma_1$  max = 94.0 MPa  
 $\sigma_2$  max = 47.0 MPa  
 (see table 2)

\* crack indication  
 ( ) crack length determined with Eddy Current

		countersunk side																															
cycles (10 <sup>3</sup> )		1	2	3	4	5	6	7	8	9	10	11	12	13	14	15	16	17	18	19	20	21	22	23	24	25	26	27	28	29	30		
		L	R	L	R	L	R	L	R	L	R	L	R	L	R	L	R	L	R	L	R	L	R	L	R	L	R	L	R	L	R	L	R
100																		*	o														
110																		*	o														
120																	4.0	o															
130																	4.5	*	2.0	o													
132.5																	5.5	1.5	3.0	o													
135																	5.5	3.5	5.5	o													
137.5																	7.0	4.0	0.5	*	o												
140																	8.0	4.5	4.5	1.5	o												
142.5																		*	3.5	4.5	4.5	3.0	o										
145								*	o	*	o	(2.0)	(2.5)	o				*	3.5	5.5	5.0	3.0	o										
147.5								*	o	(1.5)	3.0	2.5	o					o	o	o	4.5	o											
150								*	o	(2.5)	*	0.4	4.5	o			2.5	o	o	o	o	2.0	o										
152						*	o	*	1.0	*	0.2	0.5	0.4	4.5	o	*	o	*	o	o	4.5	o	o	o	6.0	o							
153					*	o	*	2.0	3.0	4.0	o	o	o	6.5	8.0	1.0	*	o	o	9.0	o	o	o	o	3.0	o							
153.317																																	

Note: All crack lengths are in mm

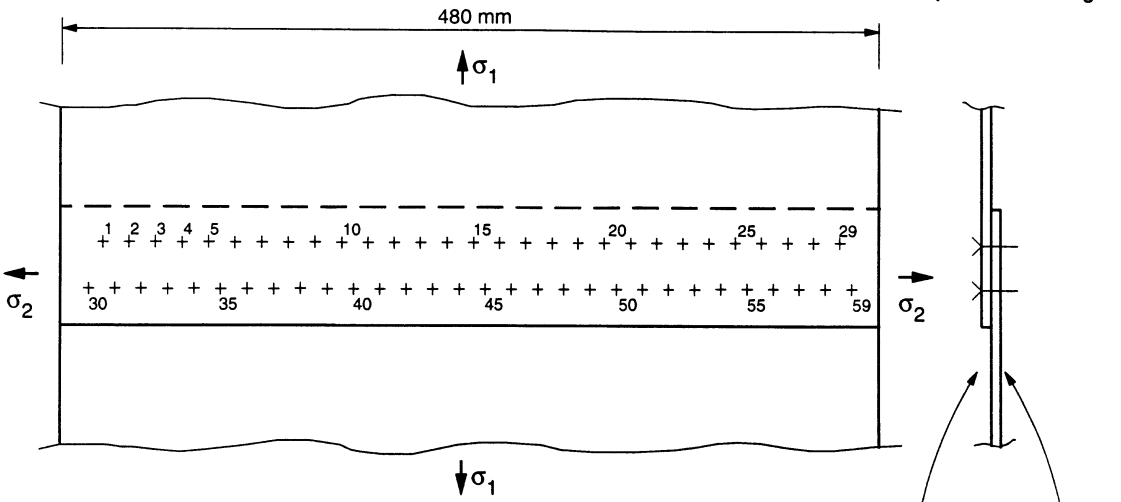
FIGURE 29. RESULTS FOR SPECIMEN D3a



Failure mode

FIGURE 29. RESULTS FOR SPECIMEN D3a (CONTINUED)

Dimensions of specimen: see figure 5a

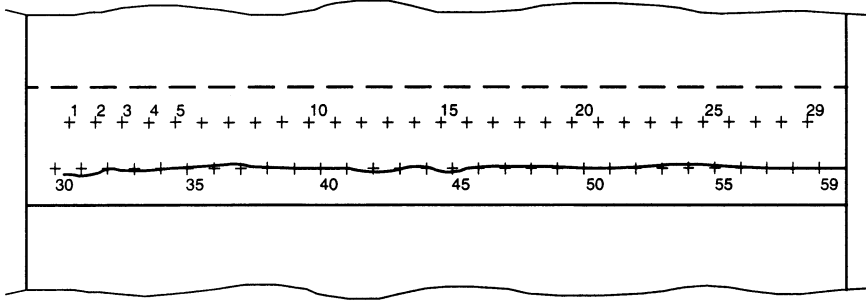


Loading: CA R = 0.1  
 biaxial  
 $\sigma_1 \text{ max} = 94.0 \text{ MPa}$   
 $\sigma_2 \text{ max} = 47.0 \text{ MPa}$   
 (see table 2)

\* crack indication

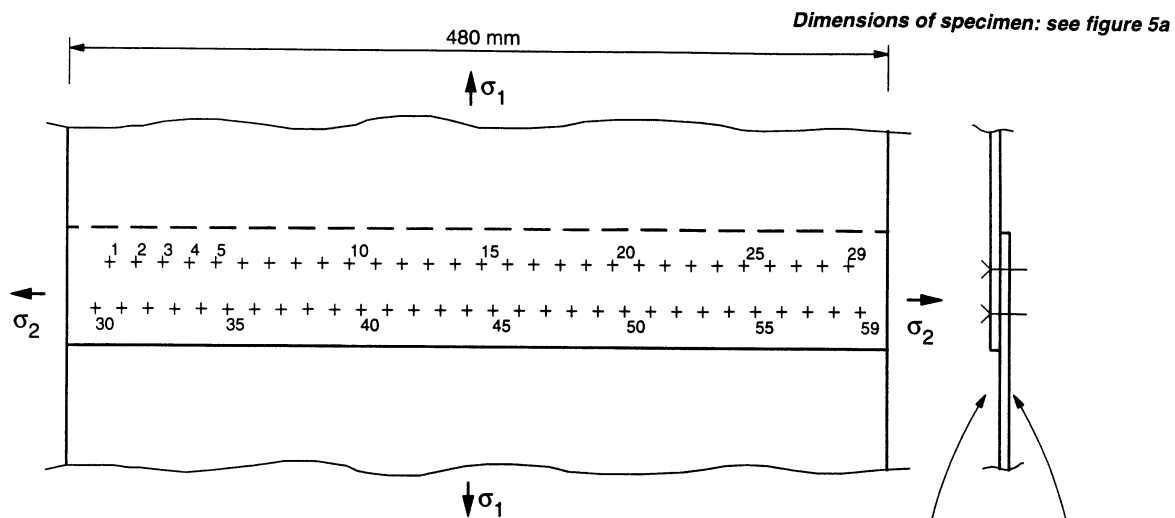
		formed head side																																							
cycles (10 <sup>3</sup> )	30	31	32	33	34	35	36	37	38	39	40	41	42	43	44	45	46	47	48	49	50	51	52	53	54	55	56	57	58	59											
	L	R	L	R	L	R	L	R	L	R	L	R	L	R	L	R	L	R	L	R	L	R	L	R	L	R	L	R	L	R	L	R	L	R	L	R	L	R			
112.5					1.0	1.0																																			
125					3.5	3.0													1.0																						
130					5.0	5.0													*3.0	2.0																					
135					*6.5	1.0													*7.0	2.0	*																				
137.48					FAILURE																																				

Note: All crack lengths are in mm



Failure mode: crack at formed head side

FIGURE 30. RESULTS FOR SPECIMEN D4a



Loading: CA R = 0.1  
 biaxial  
 $\sigma_1$  max = 94.0 MPa  
 $\sigma_2$  max = 47.0 MPa  
 (see table 2)

\* crack indication

		countersunk side																													
cycles (10 <sup>3</sup> )		1	2	3	4	5	6	7	8	9	10	11	12	13	14	15	16	17	18	19	20	21	22	23	24	25	26	27	28	29	
		L	R	L	R	L	R	L	R	L	R	L	R	L	R	L	R	L	R	L	R	L	R	L	R	L	R	L	R	L	R
106.250																															
112.500																															
118.750																															
122.500																															
124.000																															
125.000																															
125.500																															
126.000																															
126.500																															
126.706																															

Note: All crack lengths are in mm

FIGURE 31. RESULTS FOR SPECIMEN D5a



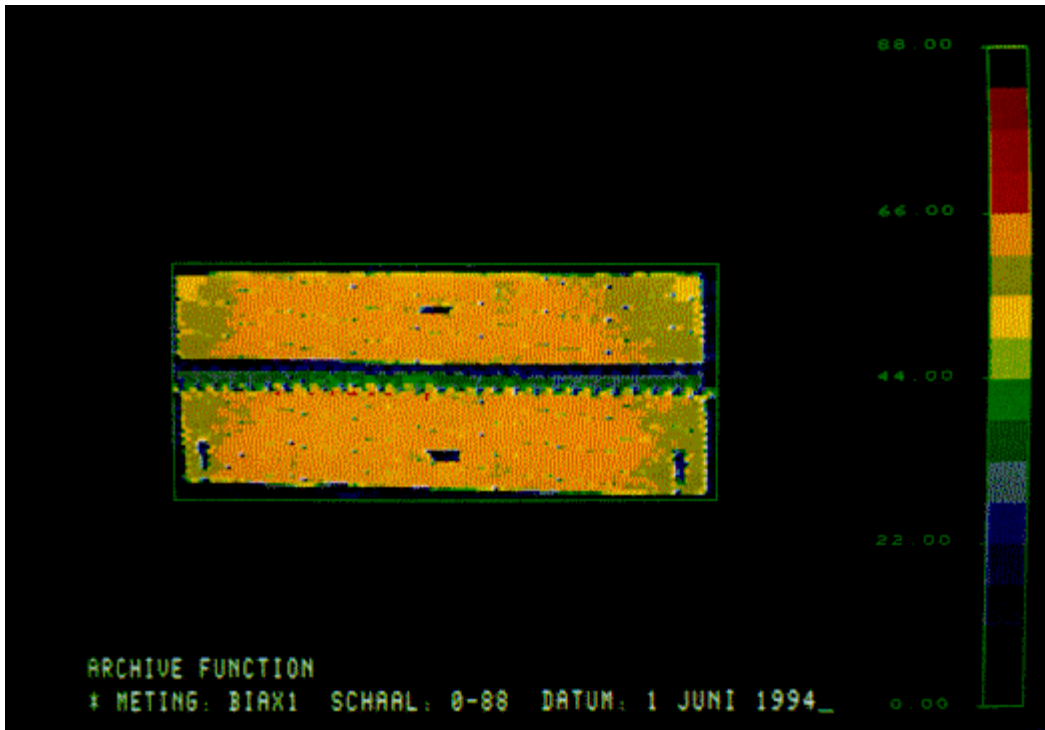


FIGURE 32. RESULTS OF SPATE MEASUREMENTS

## 7. DISCUSSION.

### 7.1 GENERAL REMARKS.

The test results show that no fatigue cracks occurred in the riveted lap joints below 500 kilocycles as long as the bonding was fully or partly intact. This conclusion holds for all riveted/bonded specimens tested whether they are uniaxially or biaxially loaded or whether they are wide or narrow.

All the specimens with degraded bonding or without bonding showed multiple-site fatigue cracking (except specimen C3a).

Some typical characteristics of fatigue crack initiation and fatigue crack growth will be discussed for specimen C1e (figure 17).

For specimen C1e the measured cracks started at rivet 18 left and at rivet 20 left. From the final crack configuration it can be seen that these cracks started at the end of the countersink near the cylindrical part. A through-the-thickness crack then developed that became visible at the outer surface as soon as it had grown outside the countersink.

At rivet 18 right and at rivet 19 left, fatigue cracks initiated at the faying surface. These cracks grew a large extent before they became through-the-thickness cracks and became visible at the outer surface.

From the fracture surface it can be seen that fatigue cracks initiated from nearly all rivet holes and that a number of cracks grew sufficiently large to cause the final specimen failure.

The data were examined to see if there was a relationship between rivet squeeze force and the location of fatigue crack initiation. The diameter of the rivet formed head is taken as a measure of the squeeze force. From table 4 the following diameters are taken:

Specimen C1e Rivet No.	17	18	19	20	21	22	23	24
Diameter Formed Head in mm	4.91	4.92	4.85	4.92	4.82	4.99	4.85	4.78

It might have been expected that a large squeeze force, resulting in a large head diameter, caused a large clamping force in the two parts. This would decrease the load transfer through the rivet and increase the load transfer by friction. In that case, crack initiation on the faying surface is more likely to occur. On the other hand small squeeze forces increase the load transfer through the rivets and then crack initiation from the end of the countersink would be more likely. Rivet 18 has one of the larger diameter formed heads: fatigue cracks started from the rivet hole at both sides and from the faying surface at the right side. Rivet 19 has one of the smallest diameter formed heads showing a similar pattern as rivet 18. Rivet 24, having the smallest formed head diameter, does not show fatigue cracking at the left side of the rivet hole at all.

It appears to be difficult and possibly impossible to relate fatigue crack initiation location directly to the riveting squeeze force indicated by rivet head diameter.

From table 3 it can be seen that the life of the specimens from inspectable crack length to failure is 20% or less of the total fatigue life. The life of the specimens from the first linkup to failure is less than 5% of the total fatigue life. These percentages are similar to those found in reference 1.

## 7.2 COMPARISON OF COUNTERSUNK RIVETED AND DIMPLED RIVETED LAP JOINTS.

The dimpled riveted lap joint specimens (D3a, D4a, D5a) have inferior fatigue properties compared to the fully unbonded countersunk riveted specimens (C4a, C5a, C6a) as is shown in the following table (taken from table 3):

<u>Specimen No.</u>	<u>Kilocycles First Crack</u>	<u>Kilocycles First Linkup</u>	<u>Kilocycles Failure</u>
D3a	120	148	153
D4a	112	135	137
D5a	112	124	127
<u>Average</u>	<u>115</u>	<u>136</u>	<u>139</u>
C4a	460	548	557
C5a	588	600	605
C6a	434	434	438
<u>Average</u>	<u>494</u>	<u>527</u>	<u>334</u>

There are two reasons for this difference. First, the dimpling process causes large plastic deformation in the vicinity of the rivet hole. This can lead to early crack initiation; in particular, initiation of circumferential cracks at the edge of the dimpled countersink. Second, the dimpled lap joint has only two rivet rows whereas the countersunk joint has three rivet rows. The loads transferred by a rivet row in the dimpled joint is higher than that for the countersunk joint.

### 7.3 THE EFFECT OF THE BONDING QUALITY.

The influence of the bonding quality on the fatigue life of the riveted and bonded lap joints was investigated. Four bonding qualities were tested:

- a. Fully bonded.
- b. Partly bonded to simulate manufacturing errors.
- c. Degradation of bonding (fully bonded, then torn apart and riveted again) to simulate bonding degradation in service.
- d. Fully unbonded.

The fully bonded and the partly bonded specimens did not fail below 500 kilocycles (see table 3) independent of the specimen width and the loading condition (uniaxial or biaxial). From these results it is concluded that as long as at least a part of the bonding is intact, for the stress level tested, fatigue of a riveted/bonded lap joint will not be a problem.

The results for the specimens with bonding degradation can be compared to the results of the fully unbonded specimens. The comparison will be made for the specimen width and the loading condition separately.

The following averaged values have been derived from table 3:

Specimen Width	Loading Condition	Bonding Degradation			Fully Unbonded		
		Specimen Numbers	First Crack (kilocycles)	Failure (kilocycles)	Specimen Numbers	First Crack (kilocycles)	Failure (kilocycles)
narrow	uniaxial	C1e, C2e, C4e	217	244	C4f	150	182
narrow	biaxial	C3e, C5e	282	330	C5f	213	263
wide	biaxial	C1a, C3a *	>612(225)	>653(307)	C4a, C5a, C6a	494	533

\*Specimen C3a did not fail.

In all cases it is observed that the specimens with degraded bonding performed better than the fully unbonded specimens. Probably the remainder of the bond gives extra friction between the two joint parts, which lead to extra load transfer by friction. Then, less loads have to be transferred by the rivets which is beneficial for the fatigue life of the joint.

## 7.4 COMPARISON OF WIDE- AND NARROW-SPECIMEN RESULTS.

The influence of the specimen width can be studied for countersunk riveted specimens that were biaxially loaded and for the different bonding conditions.

None of the fully bonded specimens, wide or narrow, failed.

For the specimens with bonding degradation, the following results were derived from table 3:

<u>Specimen Width</u>	<u>Specimen Numbers</u>	<u>First Crack (kilocycles)</u>	<u>Failure (kilocycles)</u>
narrow	C3e, C5e	282	330
wide	C1a, C3a *	225	307

\* Specimen C3a did not crack.

For the specimens without bonding the following results were obtained:

<u>Specimen Width</u>	<u>Specimen Numbers</u>	<u>First Crack (kilocycles)</u>	<u>Failure (kilocycles)</u>
narrow	C5f	213	263
wide	C4a, C5a, C6a	494	533

For the specimens tested with bonding degradation, the wide specimens had a relatively longer fatigue life from crack initiation to failure compared to the narrow specimens. In the wide specimens, cracks occurred at a limited number of rivets and not at all rivets simultaneously. It took some time before these cracks grew to such an extent that the residual strength of the specimen was substantially affected.

The comparison of the results of the unbonded specimens was somewhat hampered by the different geometry of the riveted joints. For the narrow specimen C5f, two 0.2-mm-thick aluminium foils were used erroneously instead of one foil. This led to more secondary bending in the joint which resulted in a shorter fatigue life. In the wide specimens C5a and C6a, no aluminium foil was used. This led to less secondary bending and longer fatigue life. Only specimen C4a was made correctly.

## 8. CONCLUSIONS.

Uniaxial and biaxial tests were carried out on lap joint specimens representative of the fuselage longitudinal skin splices of a commercial aircraft in which MSD has been found during operational usage. From the test results the following conclusions can be drawn:

- The dimpled, riveted lap joints show inferior fatigue properties compared to the unbonded countersunk riveted joints. The average fatigue life to failure of the dimpled

joints was about one-quarter of the fatigue life of the countersunk joints (139 kilocycles versus 532 kilocycles).

- The riveted and bonded specimens did not fail within 500 kilocycles as long as the bonding was fully or partly intact.
- The specimens with degraded bonding (bonded, torn apart, and riveted together) had a 25%-35% longer fatigue life compared to fully unbonded specimens. The remains of the bonding caused extra friction which increased the fatigue life of the lap joint.
- The small specimens (120, 160 mm) had about half the fatigue life of the wide specimens (480 mm) for the same loading condition (uniaxial or biaxial) and the same stress levels.
- The biaxially loaded specimens had a significant (35%-75%) longer fatigue life compared to similar uniaxially loaded specimens.
- It was not possible to relate the crack initiation location to the diameter of the formed rivet head (a measure for the riveting force).
- The number of cycles to crack initiation was the major part of the total number of cycles to failure. The crack growth life from inspectable to failure was at maximum 25% of the total fatigue life.

## 9. REFERENCES.

1. Vlieger, H., Results of Uniaxial and Biaxial Tests on Riveted Fuselage Lap Joint Specimens, NLR TP 94250 L, April 1994.
2. Vlieger, H., Experimental results of Uniaxial and Biaxial Fatigue Tests on Riveted Fuselage Lap Joint Specimens, NLR CR 94253 L, June 1994.
3. Heida, J.H., Eddy-Current Inspection Procedures for F28 Fuselage Lap Joint Specimens, NLR CR 92438 L.